Universität für Bodenkultur Wien
University of Natural Resources and Life Sciences, Vienna

Department of Crop Sciences
Division of Agronomy

Simulating growth and phenology of wheat in Pannonian eastern Austria using APSIM

Masterarbeit von

Wolfgang Fuchs, BSc

zur Erlangung des akademischen Grades
Diplom-Ingenieur

Betreuer: Assoc. Prof. Dr. Ahmad M. Manschadi

Mitbetreuer: Univ.Prof. Dipl.-Ing. Dr.nat.techn. Hans-Peter Kaul

19. Jänner 2016

Declaration of Originality

I hereby declare that this work was written entirely by me. I certify that information and data derived from other work, published or unpublished, are fully acknowledged in the text and references are listed in the corresponding section.

I declare that this thesis has not been submitted for an academic degree at another University or Institution.

Tulln, January 19, 2016 Wolfgang Fuchs

Acknowledgements

First of all I want to express my gratitude to Mr. Manschadi who gave me the chance to work on this fascinating topic, always answering my questions promptly, giving precise instructions, and helping wherever he could.

During the field experiment, Mr. Ivica Simonovic was an essential partner. He gave support coordinate all the various on-field measurements and necessary agricultural management options. Thanks also to Ms. Sarah Oberndorfer, Mr. Meysam Ebrahimi and Mr. Schodl for their support in the laboratory and the field.

My thanks go to all the administrative, scientific and non-scientific staff at the experimental site at Groß-Enzersdorf, Türkenschanze, and UF Tulln. Mr. Johannes Kemetter gave me friendly advice in pest management, also doing the plot sowing himself. Ms. Renate Sapik and Ms. Sylvia Zeidler supplied me with their working time for the soil sample analyses. Mr. Craig Jackson aided me to store the bulky amount of plant material. Mr. Kaul and Mr. Neugschwandtner were skilled advisors for setup of the field experiment and for scientific questions.

As a part of my studies at the BOKU, the TU Vienna, and my abroad semester in Ås, Norway, I met a range of enjoyable people. Thanks to all of you for contributing to this amazing time.

A very special acknowledgement goes to the late Professor Wolfgang Holzner. His botanical excursions to places as varied as the surroundings of the University in the city and a swamp in the Waldviertel, just to name two, impressed me during the beginning of my studies. It seemed to me that he was able to name any plant that could be found, as if he knew and understood flora perfectly. He was an exceptional teacher who made clear to me, just by fascinating me for botany, that I made the right choice studying Agriculture.

Lastly, my thanks and love go to my friends and family for the longtime friendships, awesome parties, technical support, and proofreading. Special thanks to my parents, for being inevitable support in every respect. Finally, thanks to you, Anja, for accompanying and backing me since we met and for being just as you are.

Contents

1 Introduction

Modeling is the translation of scientific knowledge into a mathematical framework. In most cases, models include simplifications and assumptions since information about the usually vastly complex systems is limited, and considering too many of their aspects leads to insolvable or highly complex models (Eck et al. 2011). Crop models are mathematical models which quantify development and growth of crops influenced by a wide range of conditions. Key components of such models are the energy input (intercepted solar radiation [$\mathrm{MJ\,m^{-2}\,d^{-1}}$]) and output (crop growth rate [$\mathrm{g\,d^{-1}}$]), duration (growing period), and accumulated crop biomass (calculated from energy input, a factor for photosynthetically active radiation PAR, and radiation use efficiency RUE [$\mathrm{g\,MJ^{-1}}$]). A minimalistic model will need at least those few calculations and variables, while more complex models might account for a range of plant stressing conditions such as pests, diseases, weeds, high and low temperatures, and limitations or excess of water and nutrients (Soltani and Sinclair 2012).

Crop models can be powerful tools for answering different kinds of questions for various purposes. However, it is important to keep in mind that crop models have limitations and cannot replace field experiments totally. Therefore, when users have studied and understood a crop model well (Soltani and Sinclair 2012), there are different reasonable applications in research (e.g. yield analysis, interdisciplinary knowledge application, assessing climate change impacts), as a tool in crop management (e.g. improving management practices, decision support for farmers, yield forecasts), and in education (e.g. farmers, students) (Boote et al. 1996; Sinclair and Seligman 1996; Soltani and Sinclair 2012).

The Agricultural Production Systems sIMulator (APSIM) is a widely recognized highly advanced farming systems model. APSIM takes genetic and environmental factors as well as management decisions into account to simulate production (crops, pastures, trees, livestock), profits, and environmental factors (e.g. nitrate leaching, soil erosion) (`www.apsim.info`, Keating et al. 2003; Holzworth et al. 2011). APSIM is driven by a generic crop model capable of simulating over 20 different crop species including wheat, maize, and soybean. Environment models deal with climate and weather, soil characteristics (e.g. pH, nutrients, water content), erosion, crop residue and others, while management models provide tools to configure management rules for specific scenarios such as variables associated with fertilization, irrigation, sowing, harvesting, grazing management, stocking rate, and intercropping. APSIM covers a wide range of application possibilities including on-farm decision-making, conceptualizing production or resource-management farming systems, supporting crop breeding strategies, evaluating risk for policy making, and adjusting management to climate change and variability (Reyenga et al. 1999; Meinke and Stone 2005; Manschadi et al. 2006; Moeller et al. 2007; Hammer et al. 2009; Huth et al. 2010).

In recent studies, APSIM has been used for quantifying the interactive effects of global warming and dimming on wheat yields and water use (Yang et al. 2013), predicting the effects of climate change on cotton yields and water use (Yang et al. 2014), and assessing the impact of climate change factors on wheat and maize crops in multi-model ensemble simulations (Asseng et al. 2013; Bassu et al. 2014).

APSIM requires a large number of parameters for initiating and running its simulation engine. The input parameters can be categorized into environmental parameters (e.g. soil characteristics, atmospheric CO_2 concentration), cultivar-specific parameters (e.g. sensitivity to photoperiod and vernalization), and management parameters (e.g. fertilization, irrigation). In order to achieve precise and reliable model simulations, it is necessary to perform adequate calibration and parameterization of the crop model. The duration of the different phenological stages determine crop biomass production and final yield. Therefore, the calibration of the cultivar-specific (genetic) parameters is a central task for achieving best crop development simulations. Parameterizing crop models with a limited set of experimental data results in highly uncertain predictions. The main factors that cause simulation uncertainty include model input data (e.g. meteorological data, soil physical characteristics, initial water and N values), model parameterization (i.e. inadequately calibrated cultivar-specific phenological development and parameterization of growth processes), model structure (poor modeling of crop growth [shoot and root] and soil dynamics [water content, nutrients, carbon biophysics]), human error in the preparation of the simulations, soil and crop parameterization, and the interpretation and presentation of simulation results (Palosuo et al. 2011; Rötter et al. 2011; Eitzinger et al. 2013; Manschadi et al. 2014). Furthermore, differences between simulated and observed data may be linked to uncertainties in the experimental data such as errors in crop and soil sampling, problems with biotic factors reducing crop growth (weeds, pests, diseases) which are usually not simulated in the models, as well as grain losses at harvest (Palosuo et al. 2011).

This gives strong reasons for the need for parameterization of particularly phenology and growth-related parameters for APSIM and crop models in general, before they can be applied with confidence. In APSIM's wheat model, ten key parameters define the genetic characteristics of a cultivar, including the different phenological sensitivity to photoperiod (`photop_sens`) and vernalization (`vern_sens`), the thermal time duration of the phenological phases from emergence to maturity, the grain number per unit stem weight at anthesis (`grains_per_gram_stem`), the maximum grain size (`max_grain_size`), and the potential daily grain filling rate (`potential_grain_filling_rate`). Zhao et al.

(2014) performed a sensitivity analysis of the APSIM *Wheat* model (yield, biomass, and day of anthesis and maturity) to cultivar-specific parameters. Their results showed that APSIM first needs to be calibrated for the phenological parameters (photoperiod and vernalization) and then for the parameters controlling grain number and growth rate in order to achieve a profound parameterization. Model parameterization based on a minimum dataset (e.g. phenological data, initial soil water content and per-layer soil characteristics, and management options [sowing date and depth, plant density, dates and amounts of fertilization and irrigation]) is generally not sufficient to predict differences in observed crop yields. Thus, a high uncertainty in simulated yields results from an insufficient parameterization dataset (Bassu et al. 2014).

2 State of the Art

2.1 Crop Modeling

Crop modeling was born about 50 years ago (Passioura 1996; Sinclair and Seligman 1996). Since then, it has undergone different maturity phases, which can be compared to living organisms (Sinclair and Seligman 1996). The first models from the infancy of crop modeling were relatively simple. Nevertheless, they provided convenient and rather user-friendly techniques to emulate interactions within complex systems. The idea of the possibility to quantify potential yield with crop models marked the transition to the juvenile stage.

Similar to a youth's extending horizon, the new technology offered new prospects to researchers: prediction of yields, reduction of experiments, evaluation of new genetic material, and much more. Many factors affecting crop growth and development were implemented in the models, consequently leading to great complexity. In addition, new findings about plant physiology were made, which contributed greatly to the required input number of parameters. Scientists realized that the increase in complexity could not go on forever and that a crop model was necessarily a highly simplified model of reality, where an uncountable number of molecular processes runs simultaneously within a single plant. As a result, the difficult balancing act of trying to model the complexity of a crop while avoiding an oversaturation of details became obvious.

During its adolescence crop modeling underwent extensive reductionism. The concept of describing processes only in basic physical, chemical, and physiological terms was driving model development, but researchers often lacked the necessary scientific understanding of underlying processes. However, the increasing complexity through reductionism did not result in more precise predictions. Awareness grew that it was impossible to create universal models, since new seasons or locations brought new challenges that were not predictable in the original model. The often heavy investment of time and resources led to very poor results.

Another finding was that models could not be validated. They do not present a single falsifiable hypothesis, but a composition of many hypotheses. Nevertheless, the attempt to validate a model can show how well it performs under specific circumstances. Users need an idea of situations where a model has proven useful – and a disclaimer for reliability in any other situation.

Once crop modeling was mature, scientists became aware of its limits. Crop models were envisioned as heuristic tools: powerful aids in research, teaching, and in applied modes. Models allow us to collect our knowledge and assumptions about a crop in an organized, logical, and dynamic framework, where wrong assumptions can be identified. In teaching, students learn by using simple and transparent models, where they can explore the main factors that influence crop production under different circumstances. In research, crop models can be used to establish concepts that reflect the current understanding. The lack of knowledge of parts of the model can uncover important but poorly understood aspects of the crop. Moreover, crop models are tools for analyzing experimental results by deducing the causes for differences between outcomes. In farm management, crop models have been used as pest management models, for instance for cotton and wheat, already in the 1980s (Sinclair and Seligman 1996).

There are two different types of crop models: mechanistic models (process-based) and empirical models. Process-based models rely on our understanding of real world processes (physical and/or physiological basis) while empirical models consist of mathematical functions chosen to fit observations (Monteith 1996). However, at lower organization levels process-based models become empirical (Sinclair and Seligman 1996; Soltani and Sinclair 2012). This becomes necessary when underlying processes are not fully understood (Passioura 1996).

Model input parameters are variables whose values are usually not changed within a simulation (e.g. radiation use efficiency of a crop). The act of finding or measuring those parameters for a specific simulation is called parameterization (e.g. for plant N simulation laboratory analysis of leaf and stem N concentration in green and senesced leaves, grain N content, and maximum N accumulation rate are required). Parameters may be estimated by using references from literature or simply by measurement. However, they should not only be "calibrated" by randomly changing values and using those fitting best to expectations, since this method does not rely on scientific understanding (Sinclair and Seligman 1996; Soltani and Sinclair 2012).

Nevertheless, there are models that include parameters which can only be determined using the model itself, by calibration. Calibration is the act of examining the model's output to support the selection of parameter values to improve the fit to observations. Calibration is seen very critically as it reduces modeling to an empirical exercise; a sole description of observations (Monteith 1996; Soltani and Sinclair 2012; Soltani and Sinclair 2015).

In a comparison of four wheat models including APSIM, researchers found that simpler models were generally more robust (i.e. fit of various indices of crop behavior between observed and simulated values) than complex models. In this study, APSIM belonged to the more complex models (Soltani and Sinclair 2015). However, according to Passioura (1996), models should be as simple as possible and require little input data.

2.2 APSIM

Described by Keating et al. (2003) and updated by Holzworth et al. (2014), the Agricultural Production Systems Simulator (APSIM `www.apsim.info`) is not only a cropping systems model but has developed into an agro-ecosystem model. APSIM consists of many sub-models for simulating biophysical processes as well as management options which are all organized by a generic simulation engine. Users can select which sub-models they want to use in their simulations and even write own models.

APSIM was developed by the Agricultural Production Systems Research Unit (APSRU) in Australia and first released in 1994. Since 2007, the APSIM Initiative (AI) manages APSIM's maintenance and development. Availability has changed from an obligatory license fee to a modified open source arrangement and free availability for non-commercial use. This has led to a sharp increase of APSIM's usage worldwide.

The initial idea of the APSIM developers was the creation of a crop model for accurate yield estimation as a result of management, combined with forecasts of long-term impacts of farming practice on the soil. 20 years later, APSIM has become a multi-purpose agro-ecosystem model used for assessing on-farm management practices, climate change adaptation strategies, mixed pasture and livestock strategies, agroforestry resource competition, nutrient leaching, gene trait expression, and many more.

2.2.1 Overview

Keys in the development of APSIM were the generic manager as well as the modular design. The inclusion of the generic manager enabled the capability of flexibly including farm management specifications, while the modular design facilitates easy inclusion (plug-in and pull-out) of versatile models, all handled by the central generic simulation engine. APSIM inherited much of its underlying science and knowledge from other models, mainly AUSIM (McCown and Williams 1989), PERFECT (Littleboy et al. 1989), and CERES (Ritchie and Otter-Nacke 1985).

APSIM's core system components are:

1. a set of biophysical models, representing scientific knowledge and (farming) management options,

2. a software framework, enabling combination of the models and data exchange between them,

3. a community of users and developers, working on and with APSIM, sharing experiences, data and source code,

4. a data platform, to ease sharing within the community,

5. and a user interface, to make APSIM user-friendly and accessible to a wide range of people.

The biophysical models (a more detailed list including references is provided in Holzworth et al. (2014)) include soil-related models and processes (such as soil water movement, water infiltration, evaporation, runoff and drainage, solute movement, soil nitrogen (N) and organic matter dynamics, soil phosphorus (P), soil pH, erosion, surface residue dynamics), plant models (a broad range including barley, canola, cotton, oats, oil palm, pasture, rice, wheat, maize, and potato), animal models (e.g. cattle and sheep), and climate models. The *Wheat* and *SoilWat* models will be explained in detail in the following sections. In addition to the rather simple *SoilWat* model, there is a more complex model named *SWIM* (Soil Water Infiltration and Movement) which is based on the Richard's equation. Despite their contrasting complexities, both soil water models, *SoilWat* and *SWIM*, are equally applicable in APSIM and give good results for soil water content and solute movement (Verburg 1996).

In general, a model represents a specific set of calculations. For APSIM, this constitutes a set of processes, e.g. a crop or water balance is a model, while photosynthesis or runoff are considered processes. APSIM models are process-based (mechanistic) and act on a daily time-step. An APSIM simulation is built by joining models together to form a larger model, where each sub-model is initialized with its own parameters. A set of toolboxes contains various biophysical and infrastructural models (Figure 1) that are used to build simulations as required.

2.2.2 Plant Models

APSIM's plant models simulate key physiological processes in response to daily weather data, soil properties, and farm management. Simulated processes include phenology, development of organs (leaf, stem, root, and grain), water and nutrient uptake, carbon assimilation, N partitioning, and abiotic stresses (e.g. shortage of water and N). Simulation of crop ontogeny uses empirically-determined crop responses to temperature (thermal time) and photoperiod. Simulation of potential crop water uptake applies relations with root exploration and extraction potential. All general and specific crop and cultivar coefficients are stored separately from the source code to enable users to easily change them if necessary.

2.2.3 The Wheat Model

APSIM's *Wheat* model (Zheng et al. 2014) simulates wheat growth and development on an area basis and at a daily time-step. The model responds to weather data (global radiation, minimum and maximum temperature, and precipitation), soil water content,

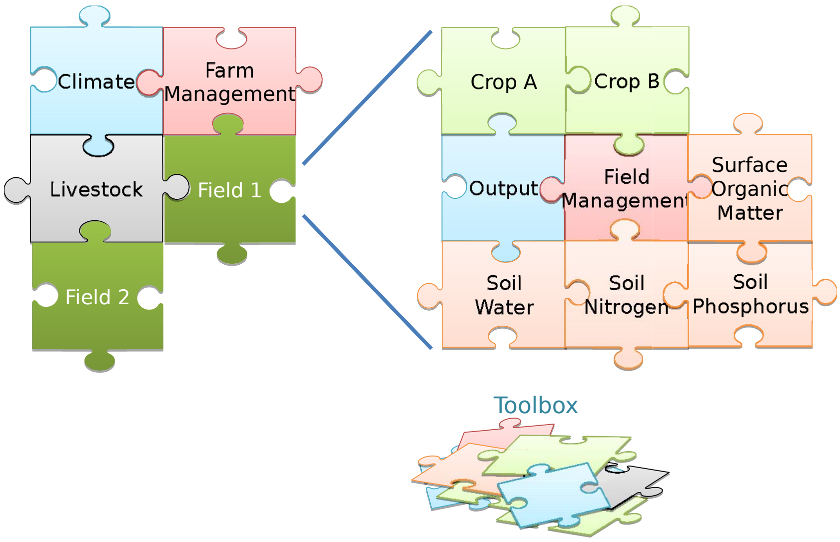

Figure 1 – A possible arrangement of an APSIM simulation, with a "top-level" farm containing two fields and livestock as well as climate and farm management models. From the graphical user interface (GUI), the models are selected from the toolboxes and added to a simulation simply by "drag&drop". The software framework, including the generic simulation engine, handles communication between the models (*APSIM & The APSIM Initiative* 2014, modified).

soil N content, and management. It communicates simulated soil water and N uptake, crop cover, and crop and root residue to the corresponding models.

Most of the model's parameters (wheat and cultivar specific) are externalized from the source code into an extensible markup language (XML) file. Almost all relations defined in this XML file are linearly interpolated by APSIM.

Some processes implemented in APSIM's *Wheat* model (such as P stress) are having no influence on the simulation by default in the current version. Most of those processes can be activated by modifying the appropriate entries in the XML file. Future versions of the *Wheat* model might have changed settings, adding some of these processes to the simulations by default.

Phenology

The *Wheat* model works with 11 phenological phases (Figure 3), which are all (except the phase from sowing to germination, which depends on sowing depth and thermal time) calculated using adjusted accumulated thermal time (TT'). Each phase has a fixed duration defined by a thermal time target (`tt_<phasename>` e.g. `tt_end_of_juvenile`), which is cultivar specific. The adjustment of thermal time accounts for factors such as vernalization and photoperiod. This means that APSIM reduces thermal time (TT' < actual thermal time), for instance during short-day conditions for photoperiod-sensitive

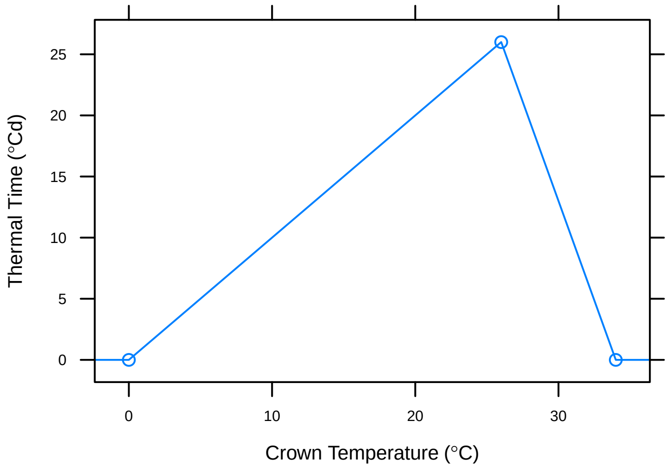

Figure 2 – Daily thermal time ΔTT in response to daily mean crown temperature T_c. Figure from Zheng et al. (2014).

cultivars, thereby increasing the duration of a phase.

The adjusted and accumulated thermal time per phase (TT') in APSIM is calculated from daily temperature as follows:

1. Input: daily minimum and maximum air temperature (T_{min}, T_{max})

   Calculation: equal for non-freezing conditions, modified at freezing conditions (also accounting for snow depth)

   Result: daily minimum and maximum crown temperature (T_{cmin}, T_{cmax});

2. Input: T_{cmin}, T_{cmax}

   Calculation: average of T_{cmin} and T_{cmax}

   Result: daily mean crown temperature (T_c)

3. Input: T_c

   Calculation: a function (Figure 2) accounting for too low and too high temperatures, where no development occurs (below 0 and above 34 °C), normal development (linear increase, 0-26 °C), and stressing high temperatures (linear decrease, 26-34 °C)

   Result: daily thermal time (ΔTT)

4. Input: ΔTT

   Calculation: summed ΔTT multiplied with vernalization and photoperiod factors (both between 0 and 1)

   Result: adjusted and accumulated thermal time per phase (TT')

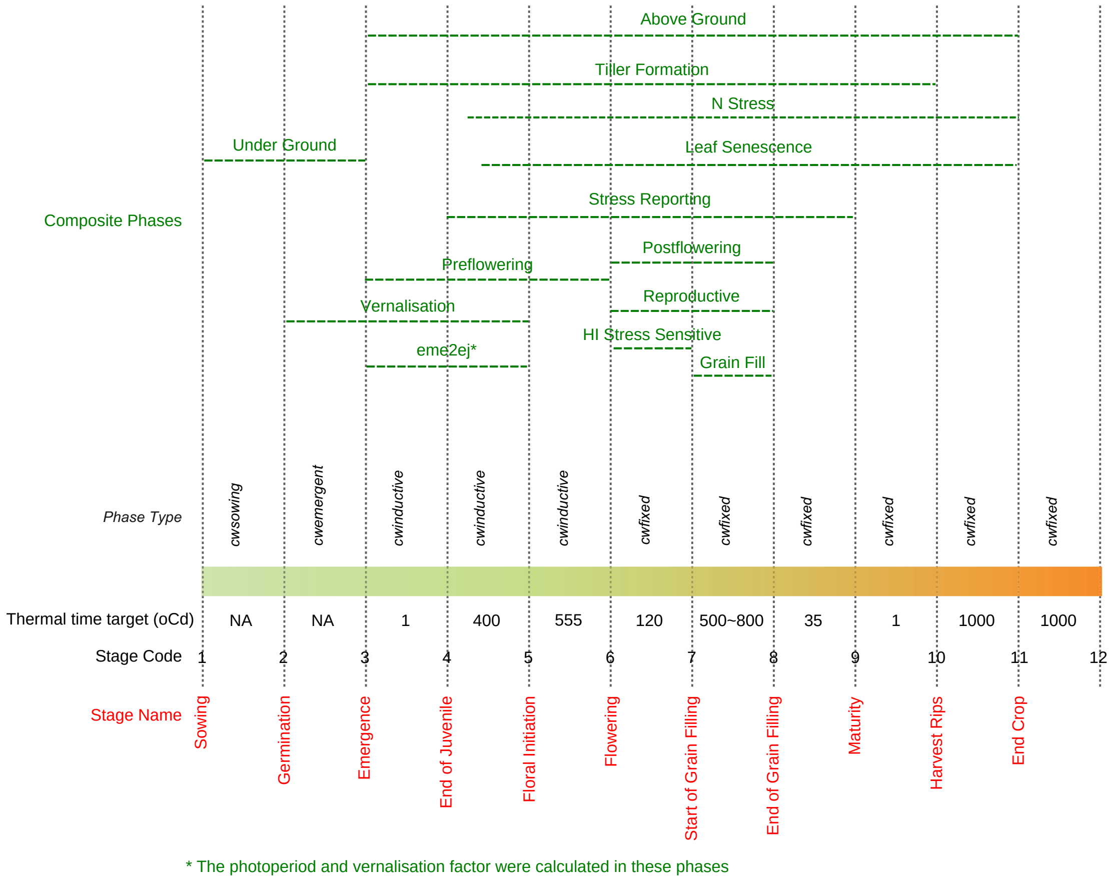

Figure 3 – The 11 phenological phases in the APSIM *Wheat* model. The exemplary values for the thermal time targets [°Cd] are given for the reference wheat cultivar *Hartog*. Figure from Zheng et al. (2014).

Environmental factors (soil water stress, N stress, and P stress) are calculated but do not affect phenology in the current version of APSIM.

Photoperiod and vernalization factors (Figure 4) both affect the duration of the phenological phases between emergence and floral initiation (Figure 3). Both include cultivar-specific sensitivity parameters (variable names: `photop_sens` for photoperiod and `vern_sens` for vernalization). Photoperiod is calculated using day of year and latitude with standard astronomical equations, vernalization uses T_c, T_{min}, and T_{max} (Figure 5). Devernalization is possible as long as cumulated vernalization is low and T_{max} above 30 °C. Cumulated vernalization (V) is the sum of daily vernalization (Figure 4b) minus the sum of daily devernalization and determines the vernalization factor which affects ΔTT (see above).

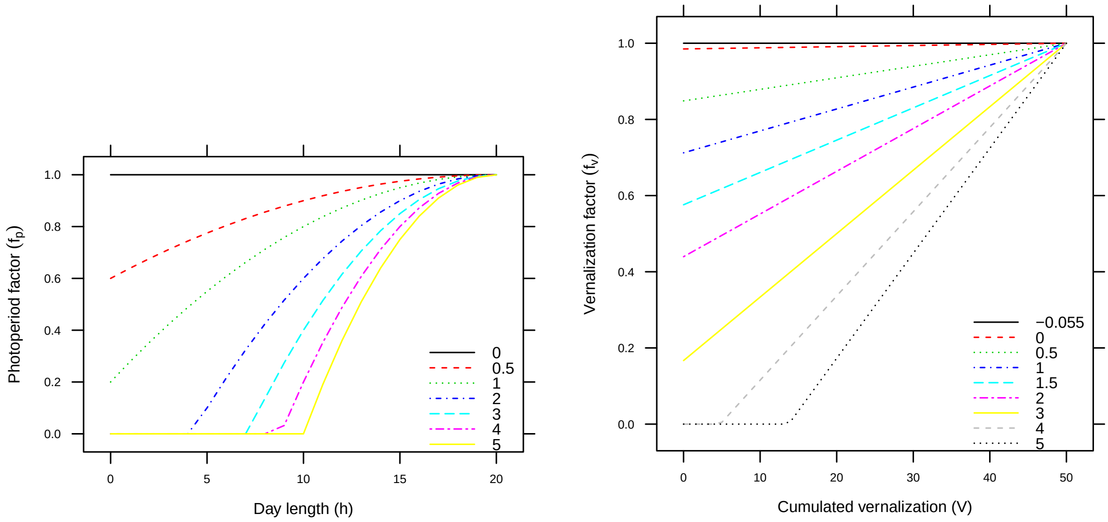

(a) **(b)**

Figure 4 – (a) Relation between APSIM's photoperiod factor and day length with different sensitivities to photoperiod (black and colored lines). The default photoperiod sensitivity is 3. (b) APSIM's relation between vernalization factor and cumulated vernalization with different sensitivities to vernalization (black and colored lines). The default vernalization sensitivity is 1.5. Figures from Zheng et al. (2014).

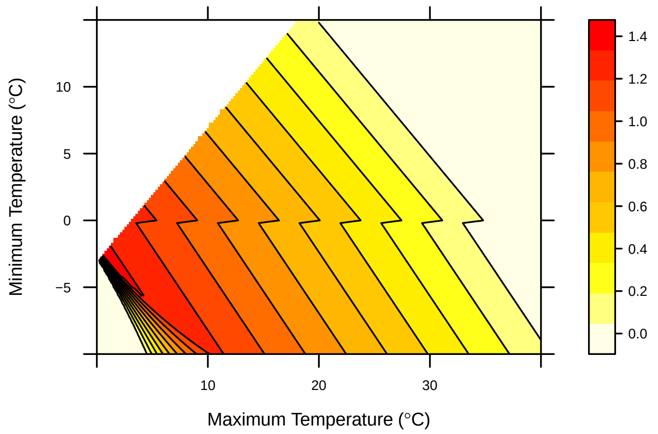

Figure 5 – APSIM's relation between vernalization (colored scale) and minimum and maximum temperature. Figure from Zheng et al. (2014).

Biomass Accumulation and Partitioning

Biomass accumulation through photosynthesis is simulated using radiation use efficiency (RUE) and radiation interception (directly taken from weather input data), limited by soil water deficiency, and modified by other factors (such as carbon dioxide factor, temperature stress factor and nutrient stress factors). Only leaves are considered photosynthetic active in the current version of APSIM. The main factors determining the potential biomass production are radiation interception and soil water supply. The soil water demand is calculated using transpiration efficiency (section 2.2.3).

The wheat plant in APSIM's *Wheat* model is divided into:

- Leaf (only leaf blades)
- Stem (including leaf sheaths)
- Head
  - Grain
  - Pod (spike without grain)
- Root

Biomass is partitioned to the different plant parts in different ratios on a daily basis, varying with the crop's phenological phase. Daily growth in root biomass is calculated from the shoot:root ratio. The above-ground biomass is partitioned hierarchically in the following order: head, leaf, stem. If supply does not meet demand, biomass can be retranslocated from the stem, especially to the grain.

Leaf Development and Expansion

The *Wheat* model assumes plants to be single-stemmed. Tillers are not simulated separately. Instead, they are represented by leaves per node as a function of node number on the main stem (Figure 6).

In APSIM's *Wheat* model, phyllochron (leaf appearance rate depending on thermal time) is related to the node number on the main stem but currently assumed constant at 95 °Cd. Phyllochron is equal for all cultivars and independent of water and N stress.

Leaf area is initialized with $200\,\mathrm{mm}^2\,\mathrm{plant}^{-1}$ and the daily rate of leaf area increase is simulated according to daily actual biomass production and the presence of stress factors (N, P [implemented, but not accounted for in this version of APSIM], and soil water). The function for the stressed leaf area incorporates a relation of potential leaf area per node to the main stem node number in order to satisfy the above mentioned single-stemmed implementation of the wheat plant in APSIM. The carbon limited leaf area uses maximum specific leaf area depending on leaf area index.

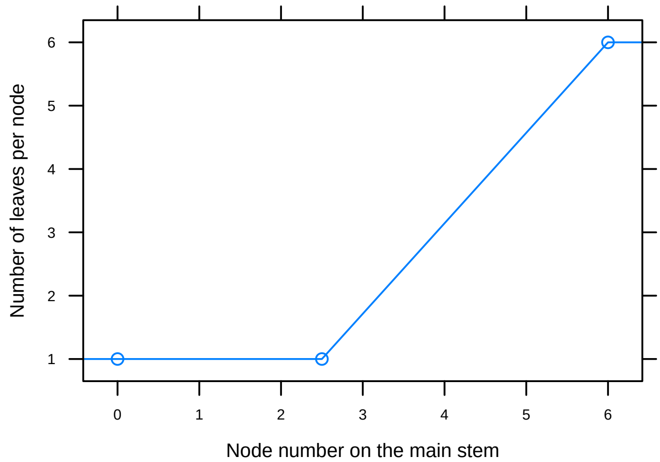

Figure 6 – The number of leaves per node as a function of the node number on the main stem in APSIM. Figure from Zheng et al. (2014).

Roots

The daily rate of root depth increase is affected by temperature, soil water content, and the soil exploration factor (XF). The root depth growth rate depends on the phenological phase, from phase 7 onwards (see Figure 3) APSIM assumes no more root growth. Too high or low an air temperature (daily mean) decrease root growth just as dry soil layers (with less than 25 % extractable soil water) do. The use of the soil exploration factor enhances consideration of soil constraints, such as compression. Root depth is necessary to calculate available soil water.

Root length growth is simulated based on growth of root biomass and specific root length. Distribution of daily root length growth to each soil layer (subsection 2.2.4) is calculated by root depth and soil water availability, also accounting for plant population density and a branching factor (XML file). Root length is only used by the root senescence process and has no effect on other traits.

Senescence

Senescence is split up into leaf number, leaf area, biomass, and root senescence. Leaf number senescence occurs at 40 % between floral initiation and end of juvenile and ends with harvest ripe (Figure 3). It is calculated using thermal time. Leaf area senescence is caused by five factors: age, dry stress, light intensity (i.e. shading), frost, and heat. APSIM uses only the daily maximum of these five factors, although frost stress is set to zero by default in the current version. However, leaf area senescence through light intensity is calculated by shading via a critical LAI (leaf area index) where shading starts to cause leaf area senescence (XML file). Heat causes leaf area to senesce to a certain ratio of LAI (Asseng et al. 2011) depending on daily maximum temperature, starting at above 34 °C, defined in the XML file. Most of leaf N is retranslocated to the stem at senescence. Leaf biomass senescence is calculated as a ratio (LAI senescence to green LAI). Roots senesce at a rate of 0.5 % per day, senesced biomass is then passed to and handled by the soil N model as fresh organic matter.

Water

Transpiration demand is simulated based on the potential crop growth rate, estimated from radiation interception and RUE, divided by transpiration efficiency (Sinclair 1986). Transpiration efficiency is a function of atmospheric vapor pressure deficit (VPD) and a stage-dependent transpiration coefficient, which is linearly related to CO_2 from 350 ppm to 700 ppm (Reyenga et al. 1999).

APSIM calculates potential (drained upper limit DUL minus lower limit LL) and actual (soil water content SW minus LL) plant extractable soil water (ESW) in all soil layers where roots are present. For soil layers that are not fully explored by roots APSIM scales ESW to the proportion of soil layer which contains roots.

The *Wheat* model may be used together with the *SWIM* or the *SoilWat* model (subsection 2.2.4). The factor KL is used to define the proportion of available soil water to be extracted per day. It is empirically determined and incorporates plant and soil factors that limit the rate of water uptake. KL needs to be defined for each combination of crop species and soil type.

The actual soil water uptake is the minimum of soil water supply and demand. This minimum might affect biomass production (section 2.2.3).

Soil water stress is simulated using soil water deficit factors. These affect photosynthesis, leaf expansion, and phenology (phenology disabled in the current version).

Nitrogen

The phenological phases between end of juvenile (at 30 % of TT target to floral initiation) and harvest maturity (Figure 3) are affected by nitrogen stress. Ammonium (NH_4^+) is not taken up in the *Wheat* model, while nitrate (NO_3^-) is. The calculation is based on soil bulk density, actual and potential ESW, depth of the soil layer, soil nitrogen concentration, and a constant for extractable soil nitrogen.

Total wheat N demand is the sum of the N demand of the plant parts leaf, stem, and pod. Each part has a defined minimum (structural), critical (plant part tries to maintain this level), and maximum (stored extra N, retranslocateable) N concentration, which depend on the phenological phase. N demand of grain starts at anthesis and is calculated based on grain number, thermal time, potential grain N filling rate, and a factor accounting for temperature, the last two are defined in the XML file. If N supply from soil N uptake and retranslocation from senescing plant parts does not meet grain

N demand, N is retranslocated from non-senesced (green) plant parts up until their N concentration drops to minimum. This way of N retranslocation is only attributed to grain.

The current version does calculate N stress for phenology, but it is not applied. However, N stress is calculated and applied for biomass accumulation and leaf appearance and expansion using actual leaf N concentration in relation to leaf minimum and critical N concentration. Thereby, radiation-limited biomass accumulation and potential leaf number as well as the stressed LAI are affected. N stress for grain filling affects both the biomass and N demand of grain.

2.2.4 The SoilWat Model

The *SoilWat* model (Probert et al. 1998; *APSIM Documentation: SoilWat* 2015) is based on the cascading, or "tipping bucket", approach. The water properties of a soil are described by the parameters LL15 (lower limit), DUL (drained upper limit), and SAT (saturated) for each horizontal soil layer, measured in volumetric water content. The user specifies the thickness of each soil layer. Commonly used thicknesses are 100 mm to 150 mm for the topmost layer and 300 mm to 500 mm for the other layers.

Processes modeled in *SoilWat* include:

- runoff, calculated using a modified USDA (United States Department of Agriculture) curve number approach, considering influence of soil water content, soil cover from crop and crop residue, and soil surface roughness due to cultivation
- evaporation, based on potential evaporation (Priestly-Taylor) influenced by crop cover or crop residue
- saturated flow, occurring in soil layers with water contents above DUL, a defined proportion (swcon) of the water in excess of DUL drains to the layer below
- unsaturated flow, occurring below DUL between layers with different soil water content
- movement of solutes, together with saturated and unsaturated flow

The initialization of soil water content can be achieved by different approaches. One is to simply set the initial soil water content for each layer manually, another to fill each layer to a fixed fraction of maximum available soil water.

2.2.5 Outlook

Since its release, APSIM has undergone continuous development. The next step is the plant modeling framework (PMF, Brown et al. 2014) which is aimed at creating models from generic crop templates at different levels of complexity. Furthermore, PMF tries to increase code reuse and minimize the amount of code that needs maintenance. Structure and parameterization of a crop model are externalized (out of the source code, into plant configuration files). A framework for easy inclusion of new models (plant organs, processes, functions) is provided.

PMF classes are divided into top-, mid-, and low-level function classes. The top-level *plant* class serves as an interface with the APSIM environment. The mid-level classes include organs (e.g. root, leaf, and others) and process classes (e.g. phenology), while low-level classes contain, for example, generic mathematical functions (such as addition, subtraction, division, etc.). Types, arrangement and parameterization of classes in a model are specified in a plant configuration file (XML, extensible markup language) making it easily accessible for non-programming developers. In addition, models can be constructed visually using the IDE (integrated development environment) approach.

Brown et al. (2014) shows that models of various complexity can be created using PMF: *Slurp*, a simple model (leaf and root organs), *Oat*, a complex crop model (including phenology), *Lucerne*, a complex model for a perennial crop that is frequently cut (reset of phenological stages after cuts), *Wheat*, another complex crop model. The current APSIM *Wheat* model is extensively validated and has a large user base that expects the same performance from a new APSIM/PMF *Wheat* model. Consequently, the current APSIM *Wheat* model has been partly transformed into PMF, meaning that a PMF *Wheat* model was created using PMF's generic classes wherever possible and additionally porting other necessary processes (code parts) from the current *Wheat* model. So far, the outputs of the PMF *Wheat* model and the existing APSIM *Wheat* model are identical, using APSIM's standard *Wheat* model valitation set (including 164 simulations at a wide range of environments and treatments).

It is obvious that re-testing a model requires considerable effort. Apparently, developers avoid making source code changes to validated models. This limits the ability to improve models and fix bugs. Therefore, PMF includes plant configuration files where the model structure is integrated. However, this solves the problem only partially. The PMF developers focus on testing the generic applicability and fix bugs instead of validating models. Nevertheless, APSIM's *Wheat* model will be evolved into PMF (Brown et al. 2014).

2.3 Model Parameterization

The process of parameterizing a crop model is commonly divided into several steps and carried out in the following sequence:

1. Phenological development
2. Soil water/nitrogen dynamics

3. Leaf development

4. Biomass production and yield formation

The following parameters need to be measured and used as inputs. They are mostly inevitable for a simulation with APSIM's *Wheat* model (parameters marked with an asterisk (*) are required for each soil layer):

- Crop phenology
  - Photoperiod and vernalization factors
- Management
  - Sowing date
  - Sowing density
  - Sowing depth
  - Row spacing
  - Crop
  - Cultivar
- Soil
  - Soil depth
  - Soil layer depth*
  - Bulk density*
  - Lower limit*
  - Air-dry lower limit*
  - Drained upper limit*
  - Saturation*
  - KL* (a factor modifying the plant's maximum daily water uptake)
  - XF* (root exploration factor)
  - A set of soil water related parameters: SWCON* (soil water conductivity), Summer/winter cona (second stage evaporation coefficient, derived from the PERFECT model [Littleboy et al. 1989]), summer/winter U (cumulative first stage evaporation, derived from the CERES model [Ritchie and Otter-Nacke 1985]), summer/winter dates, diffusivity constant and slope, soil albedo, bare soil runoff curve number, maximum reduction in curve number due to cover, cover for maximum curve number reduction

- Soil organic matter
  - Root and soil C:N ratios
  - Root weight
  - Erosion enrichment coefficients
  - Soil organic matter content*
  - FBiom* (factor for calculating the biomass pool carbon subject to decomposition)
  - Finert* (factor for calculating the biomass pool carbon not subject to decomposition)
- Initializations
  - Initial soil water and N (nitrate and ammonium)*
- Meteorological data
  - Maximum and minimum temperature
  - Global radiation
  - Precipitation

Calibration (comparison of simulation and observation, then adjustment of the parameter to fit observation) was carried out for some parameters (e.g. soil water content) in order to identify sources of errors.

3 Research Questions and Objectives

The overall objective of this thesis was to parameterize the APSIM models for simulating wheat growth and development in Pannonian eastern Austria. Given that APSIM *Wheat* has largely been developed and tested for spring wheat cultivars grown in subtropical regions, this research work was designed and carried out to specifically answer the following questions:

- Is APSIM in its default setting capable of simulating the course of phenology, biomass and yield of wheat grown in the Pannonian climate of eastern Austria?
  - Which model parameters need to be adjusted to enable APSIM simulating the phenological differences of winter and spring wheat cultivars sown at different dates?
- What are the causes of discrepancies between observed and simulated data?

4 Materials and Methods

4.1 Experimental Site

The field experiment was conducted at the Raasdorf experimental fields (east of Vienna) of the University of Natural Resources and Life Sciences, Vienna (Figure 10). Raasdorf is located in the Marchfeld plain, which is a major crop production region in the north-western part of the Vienna Basin (tectonically situated between the Alps, Carpathians, and the Pannonian Basin) (Wessely 2006). The climate at Raasdorf is Pannonian, with average annual precipitation of 538 mm a^{-1} and an average temperature of 10.6 °C. The soil at the experimental site is classified as a chernozem with silty loam in the top soil (Neugschwandtner et al. 2014; Neugschwandtner et al. 2015a).

4.2 Field Experiment

The wheat cultivars *Capo* (winter wheat, C) and *Xenos* (facultative wheat, X) were sown at five sowing dates (SD1: Sep. 26, SD2: Oct. 17, SD3: Nov. 7 in 2013, and SD4: Mar. 4, and SD5: Apr. 1 in 2014) in four replicates in a randomized split-plot design (Figure 7) with sowing date as the main plot and wheat cultivar as subplots. The plot size was 1.25 m by 10 m. The sowing density was 360 plants m^{-2} at a row spacing of 12.5 cm. Plants were fertilized with 120 kg N ha^{-1} split equally in two applications (Mar. 11, Apr. 10 in 2014). Due to dry weather conditions, the experiment was irrigated with 25 mm of water on Mar. 26, 2014. Plant protection (Table 1) and tillage (seedbed preparation with disc harrow) were carried out according to local farmer's practice and seasonal necessity. The preceding crop was barley.

4.3 Data Collection

Date and rate of emergence were recorded for each treatment at the beginning of the experiment. Crop phenology, leaf and tiller development scorings as well as sensor-based soil water content measurements were taken every week during the canopy's active growing period (i.e. from sowing to the end of November and from beginning of March to harvest in July).

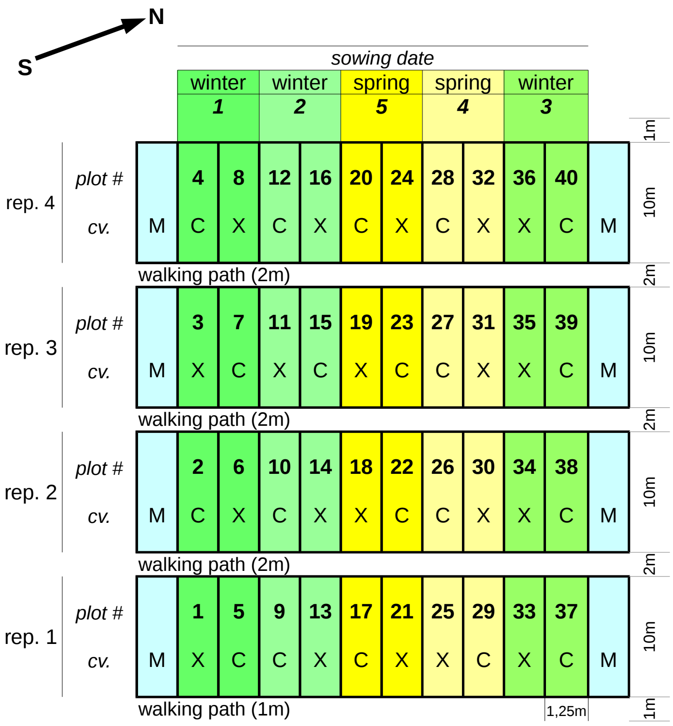

Figure 7 – Experimental layout, showing coating plots (M), replications (rep.) and wheat cultivars *Xenos* (X) and *Capo* (C). SD1: Sep. 26, SD2: Oct. 17, SD3: Nov. 7 in 2013, and SD4: Mar. 4, and SD5: Apr. 1 in 2014.

Table 1 – Plant protection measures.

Type	Date of application	Treatments	Product name	Amount [$\mathrm{l\,ha^{-1}}$]
Insecticide	31. March 2014	all	Decis	0.2
Herbicide	1. April 2014	SD1 & 2	Starane, Starane Express	0.75, 0.25
Fungicide	3. April 2014	SD1 & 2	Prosaro	1
Fungicide	13. May 2014	all	Pronto Plus	1.5
Insecticide	13. May 2014	all	Fastac	0.1
Fungicide	12. June 2014	SD4 & 5	Folicur	1

SD: sowing date, SD1: Sep. 26, SD2: Oct. 17, SD3: Nov. 7 in 2013 and SD4: Mar. 4, and SD5: Apr. 1 in 2014

4.3.1 Phenological Development

Four random plants per plot were marked soon after emergence for scoring phenology as well as leaf and tiller development. Phenology was scored according to the Zadok's Growth Scale (Zadoks et al. 1974). The total number of leaves on the main stem as well as the number of tillers (i.e. coleoptile and primary, but not secondary or higher tillers) were also recorded.

Phyllochron was calculated by fitting a linear regression to observed leaf appearance on main stem over cumulated thermal time during the phase of linear leaf appearance (i.e. from emergence to flag leaf appearance). Phyllochron was then calculated by the multiplicative inverse of the slope of the linear regression:

$$y(x) = mx + b \tag{4.1}$$

where $y(x)$ is the linear regression for the leaf number on the main stem, m the slope, x cumulated thermal time, and b the offset.

$$p = \frac{1}{m} \tag{4.2}$$

where p is phyllochron.

4.3.2 Soil Water Measurement

Soil water content measurements were done using a capacitance sensor (*Diviner 2000, ©Sentek Pty Ltd, Australia*). One PVC (polyvinyl chloride) access tube per plot was installed soon after sowing to enable measurements. Reading depth was 120 cm with 10 cm intervals, beginning at 5 cm representing the interval 0 cm to 10 cm.

The calibration process of the sensor involved multiple coupled sensor readings and gravimetric soil water content measurements in immediate proximity to each other. We tried to cover a wide range of soil conditions from very dry to very wet by choosing appropriate sampling dates (after long-lasting rainfalls and after a dry period) and sampling sites (fallow and coating plots). A regression analysis of the non-calibrated sensor readings (scaled frequencies) and gravimetric soil water content (converted to volumetric soil water content) was performed using the *LibreOffice* power function:

$$f(x) = ax^b \tag{4.3}$$

where $f(x)$ is equivalent to the sensor's (non-calibrated) scaled frequency (SF) readings and x the (gravimetric determined) volumetric soil water content Θ_g:

$$SF = a\Theta_g^b \tag{4.4}$$

The coefficients a and b of this regression analysis were then used to convert the sensor readings SF into the (calibrated) volumetric soil water content Θ_{SF}, assuming that

$$\Theta = \Theta_g = \Theta_{SF} \tag{4.5}$$

where Θ is the actual volumetric soil water content. Equation 4.4 is transformed to:

$$\Theta_{SF} = \left(\frac{SF}{a}\right)^{\frac{1}{b}} \tag{4.6}$$

4.3.3 Crop and Soil Sampling

Sequential destructive crop and soil samples were taken to determine crop biomass and leaf area development. Due to poor emergence, we did not take crop samples for SD3 except for the final harvest. Destructive crop samples during growth were taken on 21. November 2013 (SD1, SD2), and 24. March (SD1), 28. April (SD1, SD2, SD4, SD5), 19. May (SD1), 22. May (SD2), 26. May (SD4), 3. June (SD5), 10. June (SD4), and 17. June (SD5) in 2014.

Destructive crop samples of $0.25\,\mathrm{m}^2$ (0.5 m by 0.5 m) were cut immediately above soil surface and, depending on plant development, separated into senesced and photosynthetic active (i.e. green) leaf blades, stems (including leaf sheaths) and ears. A subsample of the green leaves was taken to measure leaf area (LI-3100C Area Meter, LI-COR®) and count leaf number. All samples were dried at 60 °C for 48 h and weighed.

Final destructive crop samples of $1\,\mathrm{m}^2$ (0.5 m by 0.5 m, taken four times) were cut soon after each treatment reached maturity (i.e. Zadoks stage 90), except for SD5C which failed to reach maturity until the end of July 2014. Ears were weighed, threshed and grains weighed again. Final destructive crop samples (harvest) were taken on 2. July (SD1, SD2), 16. July (SD3, SD4X), 28. July (SD5), and 30. July (SD4C) in 2014.

Soil samples for soil water content were taken to the depth of 90 cm and 120 cm using augers. For each plot, 6 to 10 samples were taken randomly, split into 10 cm intervals and mixed thoroughly. For gravimetric measurement of soil water content soil samples were packed air tight in plastic bags and cooled immediately after withdrawal to prevent water loss during transportation. Samples were then transported directly to the laboratory and weighed for fresh weight. Dry weight was measured after 48 h drying at 105 °C. Soil samples were taken on 26. September (SD1), 18. October (SD2), 8. November (SD3C), 20. November (SD1, SD2, SD3) in 2013, and 10. March (SD1, SD2, SD3, SD4), 24. March (SD1, SD2, SD3, SD4), 27. March (SD1, SD2, SD3, SD4), 2. April (all SD), 21. May (SD1, SD2), 10. June (SD4), 17. June (SD5), 2. July (SD1, SD2), 16. July (SD3), and 28. July (SD5, SD4C) in 2014.

4.3.4 Meteorological Data

The daily weather data was taken from the University's meteorological station at Raasdorf. This included precipitation, global radiation, and daily minimum and maximum temperature.

4.4 Data Analysis and Statistics

Simulations were carried out using APSIM version 7.6 (build number r3376). Analysis of variance was carried out using the GLM (General Linear Model) procedure of the SAS (Statistical Analysis System) package (Littell et al. 1991). Significant differences in the mean values were determined by Tukey's HSD (honest significant difference) test at a significance level of 0.05. Calibration of the soil water content sensor (*Diviner*) as well as parts of data processing were supported by *LibreOffice Calc* (version 4.2.8). In addition, *Microsoft Excel 2013* was used as a tool for data preparation. Figures were generated with *LibreOffice Calc*, *Microsoft Excel 2013*, and *SigmaPlot 12.5*.

5 Results

5.1 Weather Condition

The vegetation period was characterized by a very dry interval with only 22.4 mm precipitation between 11. November 2013 and 11. February 2014 (Figure 8 and Figure 9c). The following weeks until 7. April 2014 were still dry (31.4 mm), while the rest of the vegetation period, especially 8. April 2014 to 31. May 2014 (135.6 mm), was wet. Total precipitation was 272.6 mm (October-June, excluding irrigation). The winter was relatively mild (Figure 9a), with the longest period of below 0 °C average daily temperatures of exactly two weeks (21. January to 5. February 2014).

5.2 Soil Water Content

Regular soil water measurements were taken using a capacitance sensor (*Diviner*) whose default calibration equation is based on the combination of data from sand, sandy loam and organic potting soil. Using the default calibration, the measurement results are relative soil water data. In order to obtain volumetric soil water content data it was necessary to calibrate the sensor for the soil type at the experimental field at Raasdorf.

The initial idea for calibration was to use gravimetric soil water content measurements from 6 to 10 soil samples taken randomly across each plot. Using this method, correlation between sensor readings and gravimetric measurements was poor (Figure 11a). Therefore, two additional access tubes were installed each in coating plots as well as in a neighboring fallow strip. Coating plots and the fallow strip were used to cover a wide range of soil moisture contents from dry to wet, respectively. On two dates (21. May and 17. June 2014), the first after a wet two week period with a total of 57 mm precipitation (i.e. over 10 % of annual total) and the second after a dry two week period (total 0.2 mm precipitation), sensor readings and soil samples were taken. First, sensor readings were taken at least twice. Then, augers were used to take at least two soil samples in immediate proximity to the access tubes.

Soil samples from immediate proximity to the access tubes improved the correlation ($R^2 = 0.794$, Figure 11b). The coefficients of the regression analysis (see subsection 4.3.2) used for calibration of the *Diviner* sensor were $a = 0.3274$ and $b = 0.2765$ ($R^2 = 0.871$).

Calibration of the *Diviner* sensor for the field experiment's soil type resulted in little improvements of the correlation for the whole soil water content dataset (Figure 12).

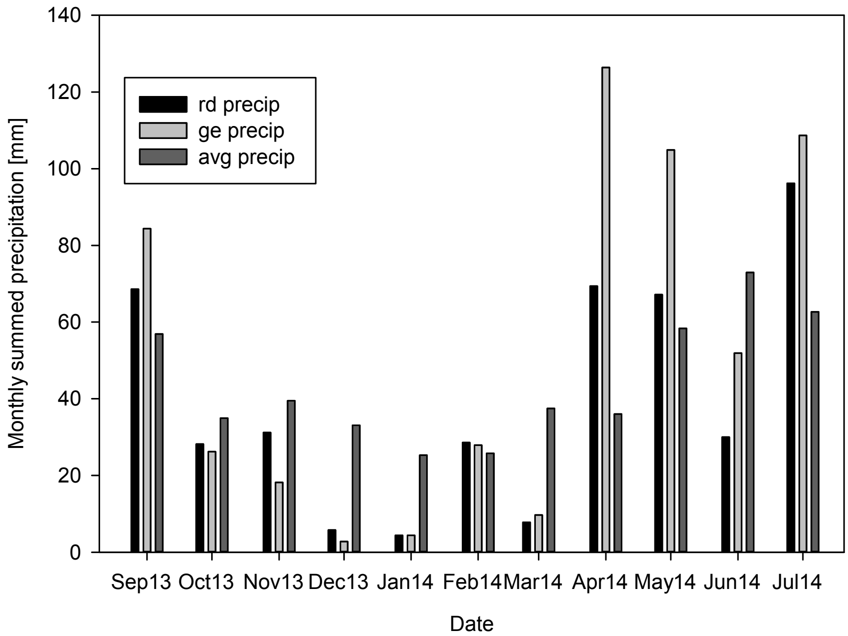

Figure 8 – Monthly summed precipitation at the Raasdorf (rd) and Groß-Enzersdorf (ge) weather stations during the wheat growing season in 2013/14 and long-term average (avg) for Groß-Enzersdorf.

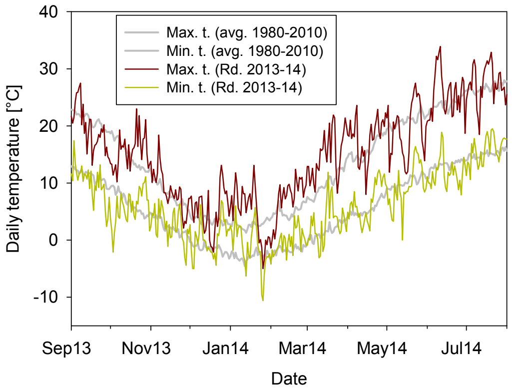

(a) Daily maximum and minimum temperature for the experiment's growing season compared to long-term (1980-2010) average.

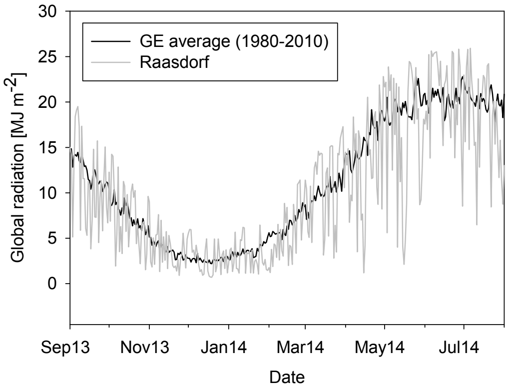

(b) Daily global radiation for the experiment's growing season at Raasdorf compared to the long-term (1980-2010) average for another weather station nearby (Groß-Enzersdorf, GE).

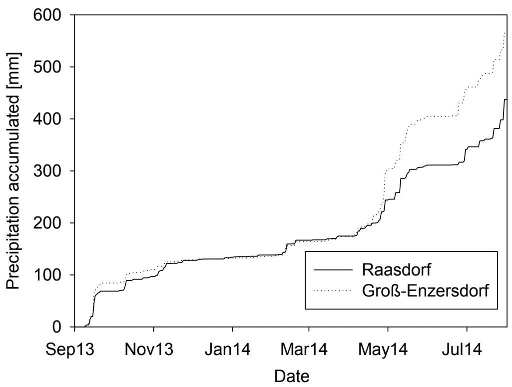

(c) Accumulated precipitation for the two weather stations close to the experimental field (Raasdorf and Groß-Enzersdorf).

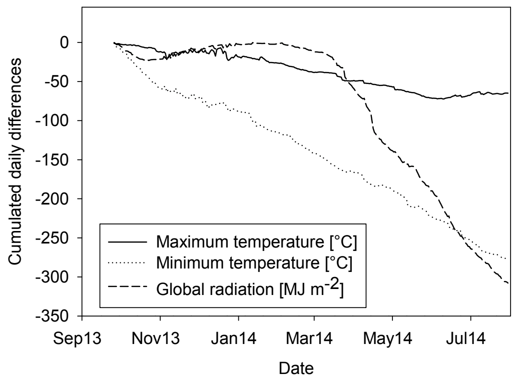

(d) Cumulated daily differences (Raasdorf minus Groß-Enzersdorf) for maximum and minimum temperature and global radiation.

Figure 9 – Various weather data for the growing season of the experiment at Raasdorf (September 2013 to July 2014).

Figure 10 – Location of the experimental field (yellow star) (*Google Maps* 2016, modified).

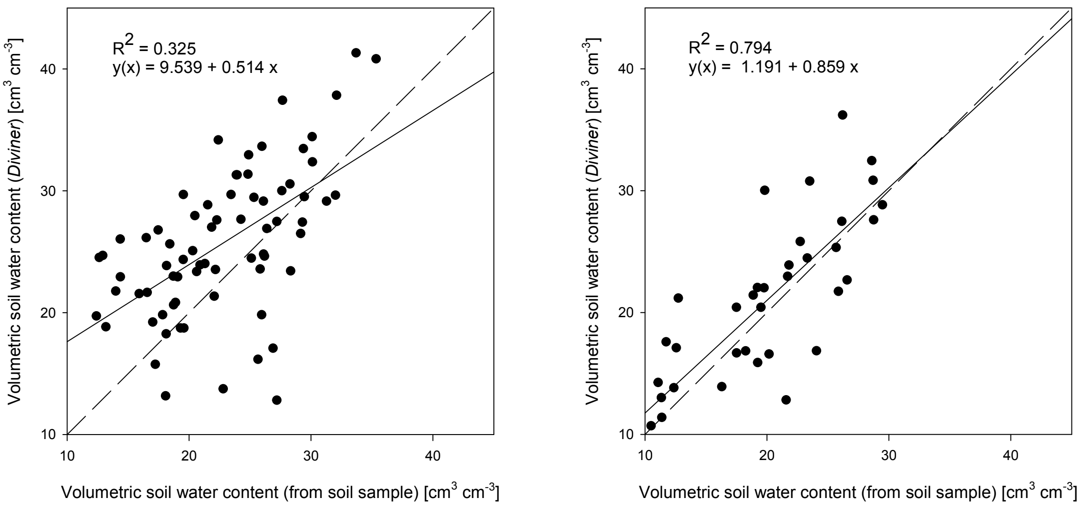

(a) **(b)**

Figure 11 – Correlation (solid line) between *Diviner*-measured (soil water content sensor) and soil sampled volumetric soil water content; soil samples taken (a) randomly across plots and (b) immediately next to *Diviner* access tubes. Dashed: 1:1 line.

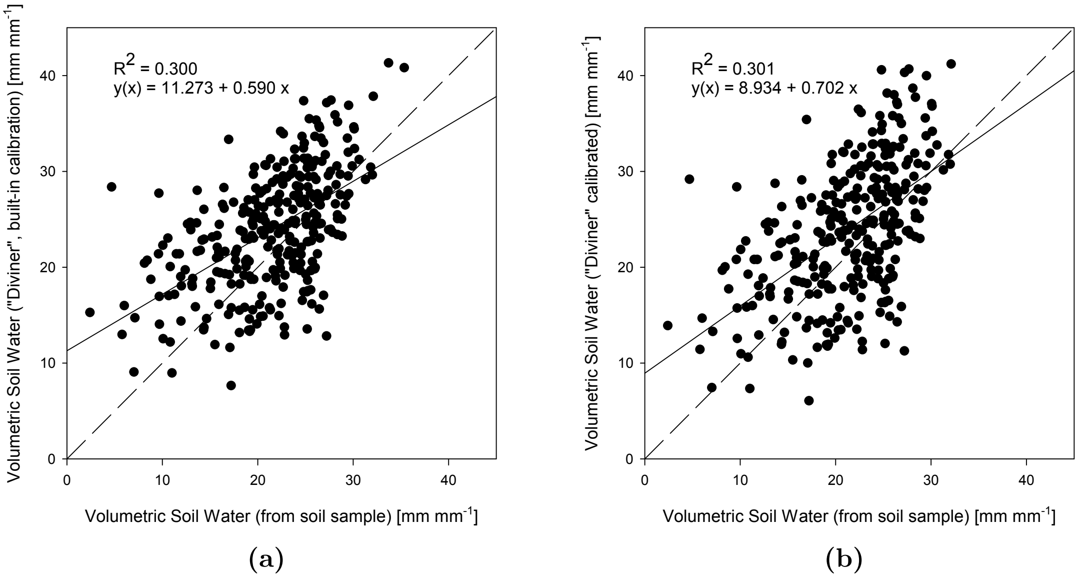

Figure 12 – Correlation (solid line) between *Diviner*-measured (soil water content sensor) and soil sampled volumetric soil water content of all collected soil water content data (a) before (i.e. using the built-in calibration) and (b) after calibration for the soil type at the experimental field (chernozem with silty loam). The built-in calibration is based on data from sand, sandy loam and organic potting soil. Dashed: 1:1 line.

Due to that improvement, although marginal, the calibrated data was used for further investigations. In addition, the correlation improved slightly when the top (0 cm to 10 cm) as well as the two deepest (100 cm to 120 cm) soil layers were removed ($R^2 = 0.339$).

5.3 Wheat Phenology, Biomass and Yield

Emergence of SD3, SD4, and SD5 was poor (Figure 14a, Figure 16), and we observed formation of a soil crust soon after sowing (Figure 17b). Up until March 2014, months after sowing of SD3, plants were still emerging (Figure 13). In mid January, many plants between Zadoks stage 05 and 09 were observed (Figure 17a).

Heavy plant damage through mice burrowing and feeding activity (Figure 14b) was observed in different plots, starting in early November 2013 throughout the whole season. Toxic mouse baits were laid out regularly, and a perch to attract birds of prey was installed. Despite those pest regulation measures, mice activity continued up until harvest.

Frost damage on leaf tips (necrotic) of SD1 and SD2, particularly for *Xenos* but also

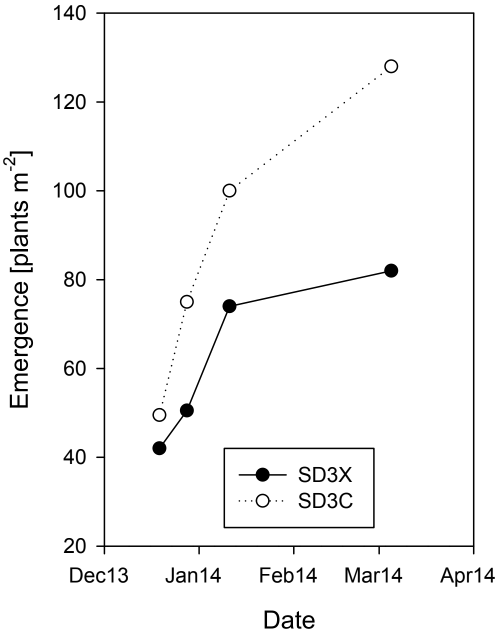

Figure 13 – Development of averaged observed emergence for sowing date 3 (7. November 2013). X: facultative wheat cultivar *Xenos*, C: winter wheat cultivar *Capo*.

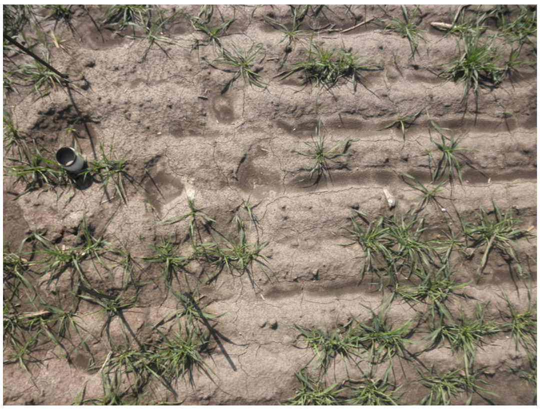

(a)

(b)

Figure 14 – (a) Poor emergence of sowing date 3 (7. Nov. 2013), picture taken on 28. Mar. 2014. (b) Typical mouse feeding damage in mid April 2014 (showing a marked plant with the labeled leaves number 8 and 9).

Table 2 – Wheat grain yield and final total aboveground biomass in $g\,m^{-2}$.

	SD1	SD2	SD3	SD4	SD5
Yield *Capo*	722	607	558	260	-
Yield *Xenos*	658	531	544	520	433
Biomass *Capo*	1926	1720	1502	984	558
Biomass *Xenos*	1665	1433	1404	1222	959

SD: sowing date, SD1: Sep. 26, SD2: Oct. 17, SD3: Nov. 7 in 2013, and SD4: Mar. 4, and SD5: Apr. 1 in 2014

Capo, was observed (November and December 2013).

We observed different leaf orientations for the two wheat cultivars, most apparent in early stages up until stem elongation. *Capo* showed a horizontal orientation, while *Xenos* leaves were vertical.

Beginning of anthesis (Zadoks 61) was observed between 14. May and 28. June 2014. SD1, SD2, and SD3 (both cultivars) started anthesis between 14. May and 28. May 2014. For SD4, *Xenos* (facultative wheat) started anthesis on 7. June, while *Capo* (winter wheat) started anthesis 21 days later (28. June). For SD5, *Xenos* flowered on 15. June, while *Capo* did not reach that stage. Final harvests were performed on 2. July (SD1 and SD2), 16. July (SD3 and SD4X), 28. July (SD5), and 30. July (SD4C).

Observed grain yields and aboveground biomass at harvest ranged from $260\,g\,m^{-2}$ to $722\,g\,m^{-2}$ and $558\,g\,m^{-2}$ to $1926\,g\,m^{-2}$, respectively (Table 2, Figure 15). Sowing date and cultivar had highly significant ($p < 0.001$) effects on yield, and the interactions were also statistically significant (Table 3). Moreover, final biomass was influenced by the sowing date ($p < 0.001$), but not by the cultivar, with significant interactions. When checking the effect of the cultivar within each sowing date, yield ($p < 0.01$) of SD4 and yield ($p < 0.001$) and biomass ($p < 0.01$) of SD5 were significantly influenced.

Strong rust fungus infestation (especially *Puccinia striiformis*, Figure 18) occurred in all *Xenos* plots of SD1 in mid March. Another rust fungus infestation was observed in almost only *Xenos* plots of SD1 and SD2 from beginning to mid May. SD3X showed first signs of rust in mid May, SD4X and SD5X in mid June.

We monitored dry stress in all, but especially *Capo*, SD1 and SD2 plots in mid March. Leaf tips were chlorotic and turned necrotic later.

In mid May, many plots of almost only *Capo* in SD1 and SD2 started lodging, but ongoing stem elongation cleared almost all lodged plots until beginning of June.

Table 3 – ANOVA results for the effects of sowing date and cultivar on wheat grain yield and final total aboveground biomass.

Source	DF	Type III SS	Mean Square	F Value	Pr >F
Dependent Variable: Yield					
SD	4	1075301.900	268825.475	39.68	<.0001
Gen	1	115885.225	115885.225	17.11	0.0003
SD*Gen	4	414494.900	103623.725	15.30	<.0001
Dependent Variable: Biomass					
SD	4	5365757.847	1341439.462	43.03	<.0001
Gen	1	25.552	25.552	0.00	0.9774
SD*Gen	4	755441.424	188860.356	6.06	0.0011

SD: sowing date, Gen: genotype (cultivar)

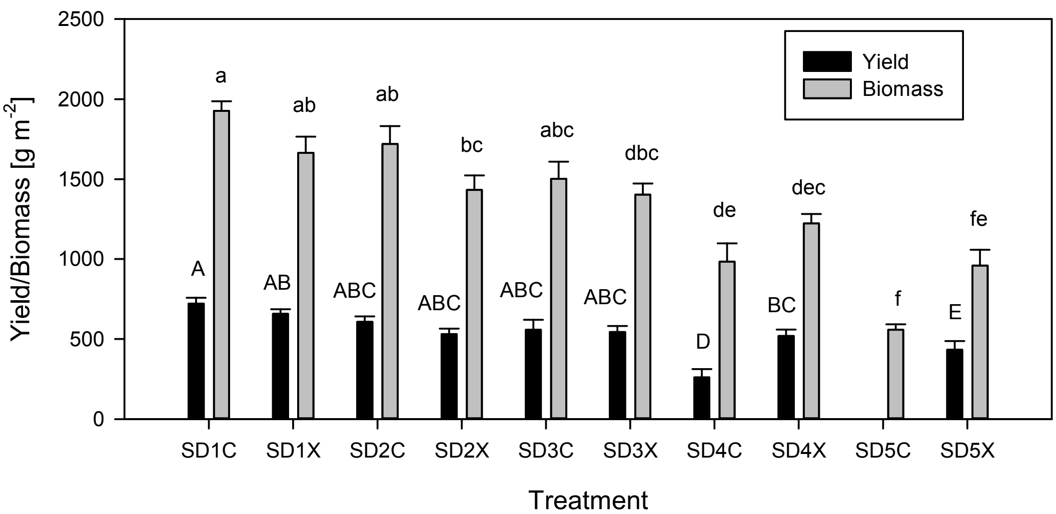

Figure 15 – Grain yield and final total aboveground biomass at harvest (mean values) of all 10 treatments in [g] dry matter per [m^2]. Error bars indicate standard errors. SD: sowing date, C: wheat cultivar *Capo*, X: wheat cultivar *Xenos*, SD1: Sep. 26, SD2: Oct. 17, SD3: Nov. 7 in 2013, and SD4: Mar. 4, and SD5: Apr. 1 in 2014. Bars with the same letter are not significantly different ($p = 0.05$).

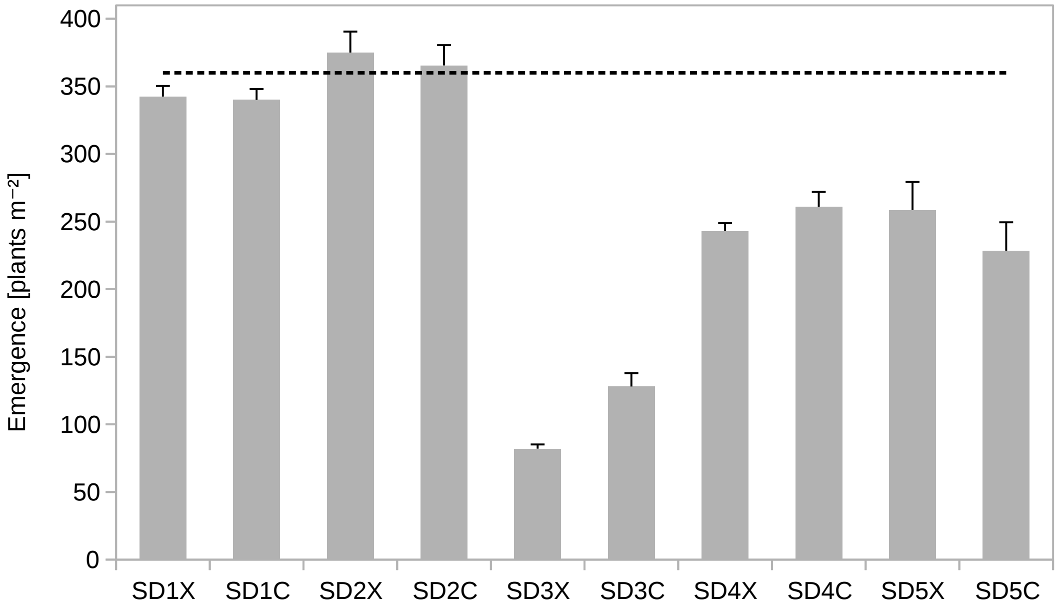

Figure 16 – Emergence rates of all treatments. Dashed line indicates sowing density of 360 plants m^{-2}, error bars represent standard errors. SD: sowing date (SD1: Sep. 26, SD2: Oct. 17, SD3: Nov. 7 in 2013, and SD4: Mar. 4, and SD5: Apr. 1 in 2014), X: facultative wheat cultivar *Xenos*, C: winter wheat cultivar *Capo*.

(a)

(b)

Figure 17 – (a) Extracted seedlings of sowing date 3 (7. Nov. 2013) which have still not emerged two months after sowing. (b) Seelding emerging through crack in soil crust in February 2014.

(a) **(b)**

Figure 18 – Heavy infection of leaves with *Puccinia striiformis* of the wheat cultivar *Xenos* in (a) mid May 2014 (sowing date 2 on 17. October 2013) and (b) mid June 2014 (sowing date 5 on 1. April 2014).

5.4 APSIM Parameterization

Due to the poor emergence of some treatments (Figure 16) we initialized APSIM with the actual emergence instead of sowing density.

5.4.1 Phenology

Simulated and observed phenological development (Zadoks growth stages) were compared visually by plotting observed versus simulated data. To improve the simulations, the wheat cultivars used in this experiment (*Xenos* and *Capo*) were added to the list of cultivars in APSIM's wheat XML file. The parameters for sensitivity to vernalization (`vern_sens`) and photoperiod (`photop_sens`) are not related to a measurable variable but are APSIM specific. Therefore, they had to be calibrated by trial and error to achieve the best match between simulated and observed phenological development. Moreover, the parameters defining certain phase durations (`tt_end_of_juvenile`, `tt_floral_initiation`) were also determined using the trial and error principle but starting values were derived from previous experiments at the location (unpublished) (Table 4).

5.4.2 Canopy Development

Observed phyllochron (Figure 19) values were 122 for SD1X, 125 for SD1C, 114 for SD2X, 112 for SD2C, 82 for SD3X, 91 for SD3C, 86 for SD4X, 103 for SD4C, 101 for SD5X, and 130 for SD5C.

APSIM assumes phyllochron to be 95 °Cd constantly (section 2.2.3) but then modifies

Table 4 – List of cultivar-specific parameter values used for the wheat simulations. These parameters are defined in the *Wheat* XML file. Parameters not mentioned here were inherited from the base_cultivar.

Parameter	Variable name in APSIM	*Xenos*	*Capo*
Vernalization sensitivity	`vern_sens`	1.5	5.0
Photoperiod sensitivity	`photop_sens`	4.6	4.9
TT emergence to floral initiation	`tt_end_of_juvenile`	380 °Cd	380 °Cd
TT floral initiation to flowering	`tt_floral_initiation`	520 °Cd	520 °Cd

Xenos: facultative wheat cultivar, *Capo*: winter wheat cultivar

TT: thermal time

it almost linearly for spring sown treatments (data not shown) and twice for autumn sown treatments (expressed as a sudden increase in the graph, e.g. for SD2 at 500 °Cd in Figure 19a; the second kink where the graph flattens marks the end of leaf development, i.e. the flag leaf has emerged). This behavior was not observed (phyllochron was constant for all treatments except SD4C and SD5C). Final leaf numbers on the main stems were (simulated vs. observed average) SD1X: 13.6 vs. 12, SD1C: 15.3 vs. 12.6, SD2X: 11.4 vs. 11.2, SD2C: 12.4 vs. 11.8, SD3X: 10.8 vs. 11.9, SD3C: 11.1 vs. 11.4, SD4X: 9.1 vs. 9.5, SD4C: 13.6 vs. 13.6, and SD5X: 9.4 vs. 9.4. SD5C had not finished leaf appearance (neither simulation nor reality) when the experiment was harvested.

5.4.3 Soil Water Content

The parameterization of soil water content and biomass trends are obviously closely related since biomass affects leaf area which has a large impact on transpiration and, therefore, water uptake. Hence, parameterizing soil water dynamics requires continuous parallel checking of biomass growth.

Initial soil water content was parameterized for each 10 cm interval of the whole profile (120 cm depth) for all 10 treatments. Values for drained upper limit and lower limit for each layer were estimated from observed soil water content (Figure 22). The initial soil water content values for simulation were set according to gravimetric and/or sensor measurements performed closest to sowing date. Simulations were then compared to observed soil water trends, and initial soil water was adjusted to match the observed trends best.

From the two different observations at hand, gravimetric measurements and sensor readings, both were used for parameterization. For each case where significant differences occurred it was decided separately which dataset to use, except for the topmost layer where only gravimetric data was used. As a result, simulations of one treatment might match gravimetric measurements in one layer and then match sensor readings in an

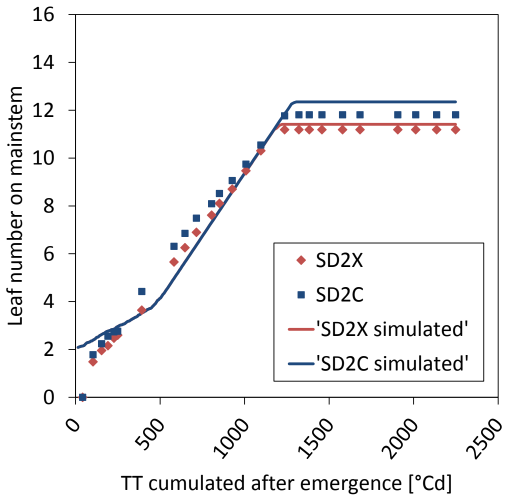

(a)

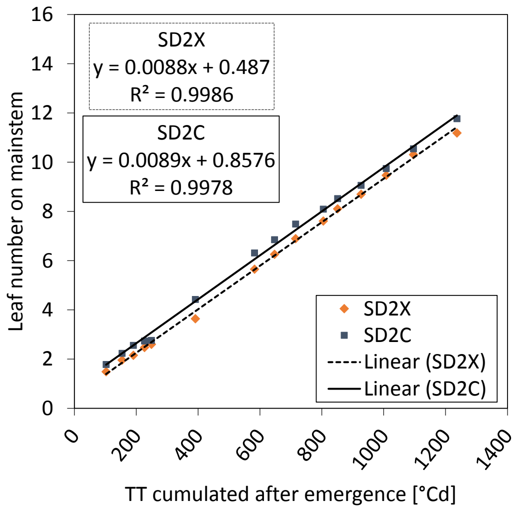

(b)

Figure 19 – Leaf number on the main stem over cumulated thermal time (TT) of SD2 (a) from emergence to harvest (lines: simulations) and (b) from emergence to end of leaf appearance (lines: linear regressions). Dots represent observations. SD: sowing date, X: facultative wheat cultivar *Xenos*, C: winter wheat cultivar *Capo*, SD2: 17. October 2013.

adjacent layer. The main basis for deciding which dataset to use was consistency of soil water gradient with neighboring soil layers.

Soil water content simulation of the topmost soil layer (0 cm to 10 cm) was poor for all treatments. Especially *Diviner* readings were hardly matched by simulated trends and absolute values, while gravimetric data fit better, although difficult to compare since they included far fewer measurements (Figure 20a, Figure 21a). We used summer cona 5 (default: 3.5) which improved the simulation of the top (0 cm to 20 cm) layers marginally. Wheat KL values used were (starting with the top layer): 0.1, 0.1, 0.08, 0.08, 0.05, 0.05, 0.05, 0.05, 0.04, 0.03, 0.03, and 0.03. Additionally, we changed `initial_root_depth` in the *Wheat* XML file to 50 mm (default: 100 mm). This change minimally improved the soil water content simulations and was kept since it also better reflects real world conditions.

In the following sections, results for sowing date 17. October (SD2) and 4. March (SD4) for the cultivar *Xenos* are presented exemplarily.

Sowing Date 17. October, Cultivar Xenos (SD2X)

Two contrary phases were found for the layers 10 cm to 40 cm (Figure 20 b, c, d). In the first phase from sowing to about 7. April, simulated trends and absolute values matched observations very well. In the second phase until crop harvest, soil water content was overestimated. Still, the simulated curve ran parallel to the measurements between 20. May and crop harvest. Very similar results were observed in all other treatments.

The layers 50 cm to 80 cm (Figure 20 f, g, h) were initialized using gravimetric sampled data. Simulations show an increase in soil water content between sowing and beginning of March (winter). This did not match the trends measured with the *Diviner* sensor, where soil water content remained constant. Nevertheless, the dates at which the decrease started agreed well in those layers as well as the 40 cm to 50 cm (Figure 20e) and 80 cm to 110 cm (Figure 20 i, j, k) layers.

The deepest layer, 110 cm to 120 cm (Figure 20l), showed unclear results. The simulations slightly overestimated soil water content compared to gravimetric measurements, though there were only three of them, unequally spread. In contrast, *Diviner* measured higher soil water contents at a constant level with a slight decrease between April and crop harvest (except for one outlier).

Sowing Date 4. March, Cultivar Xenos (SD4X)

Simulation of the top soil layer (0 cm to 10 cm, Figure 21a) hardly matched sensor readings, while gravimetric measurements fit very well.

The two phases described for SD2X in the previous section applied here as well, but only for the layers 10 cm to 30 cm (Figure 21 b, c). In addition, the mismatch was shifted in the 20 cm to 30 cm layer, with an underestimation compared to the sensor readings in the first phase (sowing to May) and a very good match afterwards.

Good matches of gravimetric and sensor measurements as well as simulations were achieved for the layers 30 cm to 70 cm and 110 cm to 120 cm (Figure 21 d, e, f, g, and l, respectively). However, between 70 cm and 110 cm (h, i, j, k), the simulation curve runs only through or close to the gravimetric measured points, while sensor readings are much higher. Still, the shapes of the curves agree with each other.

5.5 APSIM Simulation Results

The simulations were run based on the parameterization for wheat and soil water dynamics presented in the previous section.

APSIM simulated phenology very well (Figure 24). Especially the dates of anthesis were predicted with a high degree of accuracy ($R^2 = 0.962$, Figure 23).

The simulated dates of emergence were always earlier than the observed ones. There were no differences between the cultivars. Deviations for SD1, SD2 & SD5 were three days or less, SD4 and SD3 emerged 8 days and 26 days, respectively, too early in the model's predictions.

The initiation of tillering of both cultivars was underestimated in autumn (SD1 & SD2) but precise for the other SD. We tried to improve tiller initiation simulation in autumn

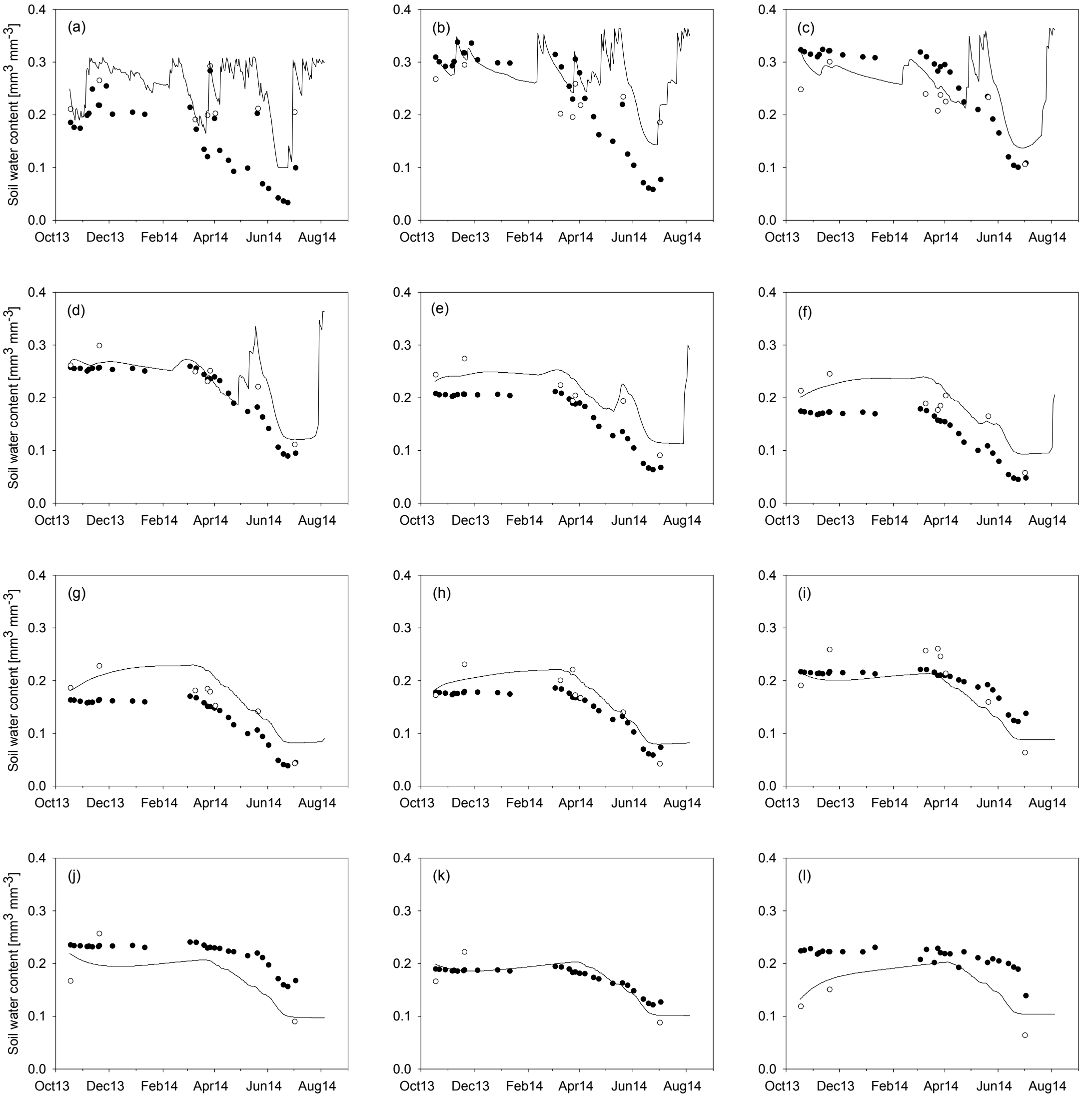

Figure 20 – Simulated versus observed soil water content for the facultative wheat cultivar *Xenos* from sowing date 2 (17. October 2013). (a) to (l) show all soil layers (0 cm to 120 cm in 10 cm intervals) in consecutive order. Lines: Simulations, symbols: observations (closed symbols: sensor measurements [*Diviner*], open symbols: gravimetric measurements [converted to volumetric soil water content]).

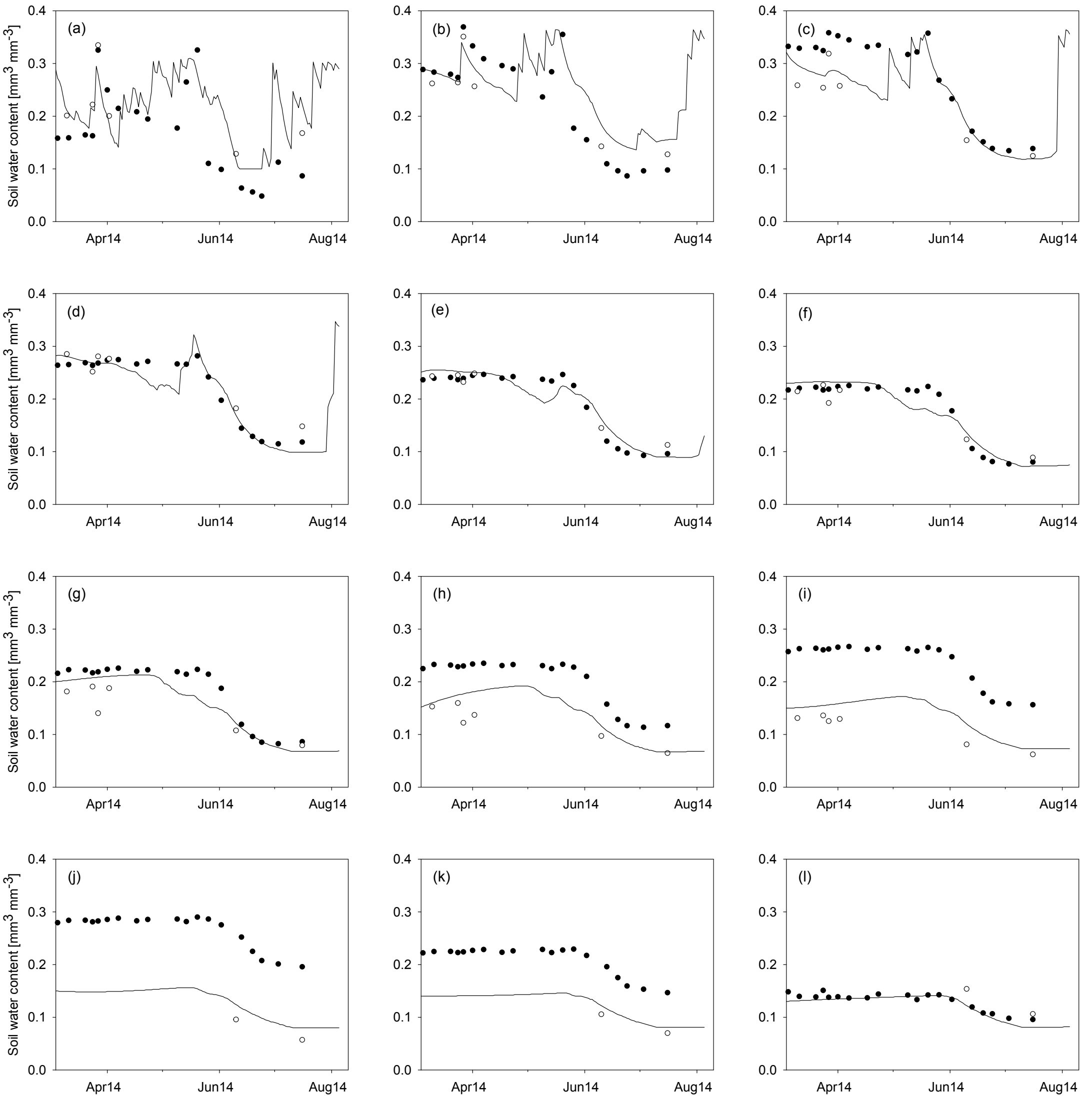

Figure 21 – Simulated versus observed soil water content for the facultative wheat cultivar *Xenos* from sowing date 4 (4. March 2014). (a) to (l) show all soil layers (0 cm to 120 cm in 10 cm intervals) in consecutive order. Lines: Simulations, symbols: observations (closed symbols: sensor measurements [*Diviner*], open symbols: gravimetric measurements [converted to volumetric soil water content]).

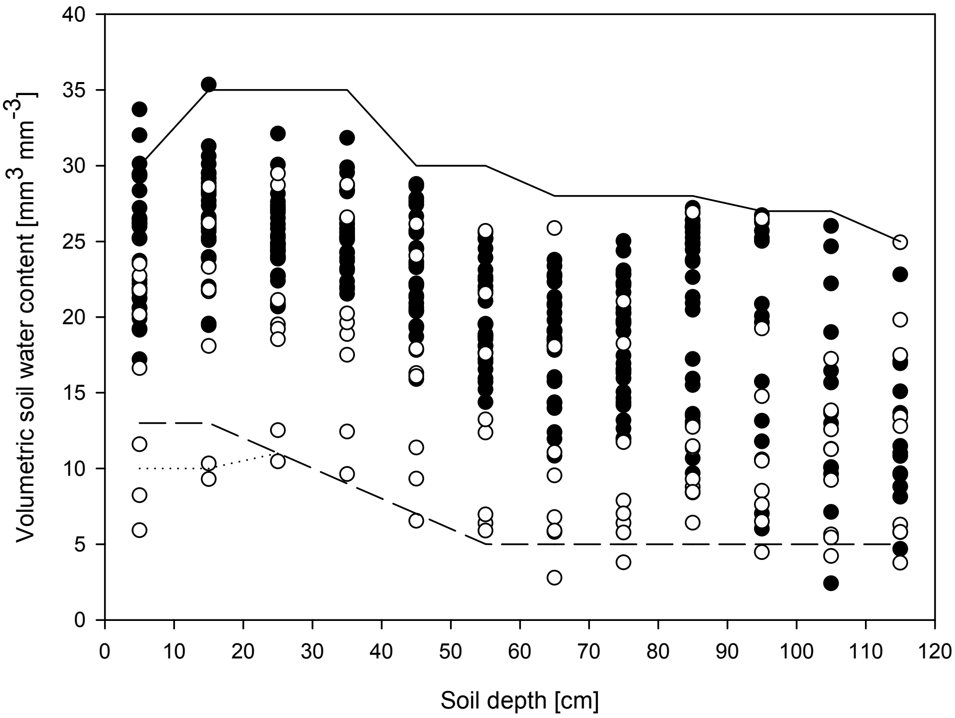

Figure 22 – Soil water content measurements (symbols) compared to drained upper limit (full line), lower limit (dashed line) and air-dry lower limit (dotted line) used in APSIM. Closed symbols represent regular measurements during the field experiment, open symbols show additional measurements to cover wet and especially dry conditions which were used for *Diviner* calibration.

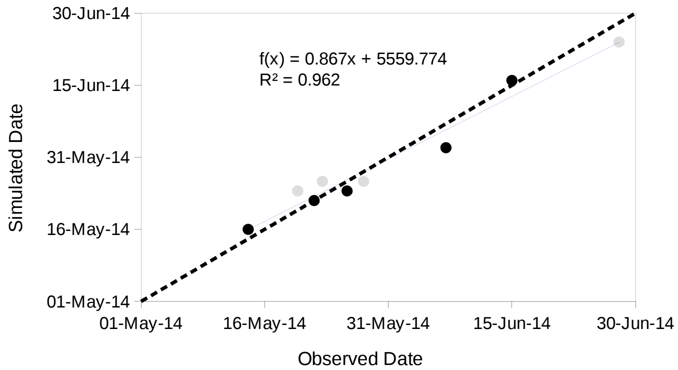

Figure 23 – Observed versus simulated dates of anthesis for the wheat cultivars *Capo* (grey) and *Xenos* (black). Dashed: 1:1 line.

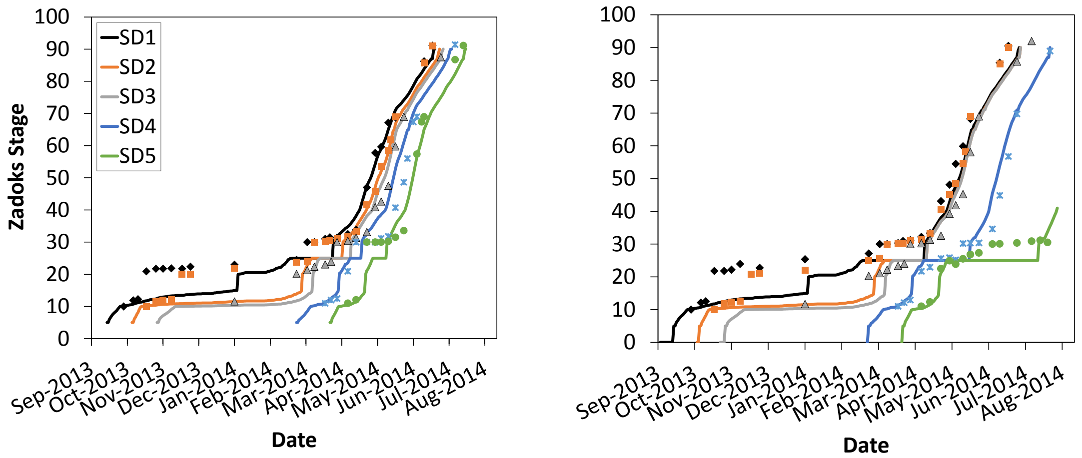

(a) (b)

Figure 24 – Simulated (curves) and observed (points) Zadoks stages of the wheat cultivars (a) *Xenos* and (b) *Capo*. SD: sowing date (SD1: Sep. 26, SD2: Oct. 17, SD3: Nov. 7 in 2013, and SD4: Mar. 4, and SD5: Apr. 1 in 2014).

Table 5 – Observed and simulated total aboveground biomass ($\mathrm{g\,m^{-2}}$) on 21. November 2013.

	SD1C	SD1X	SD2C	SD2X
Observed	50.17	58.14	14.06	11.86
Simulated	28.59	28.59	7.66	7.54
Underestimation	43 %	51 %	46 %	36 %

SD: sowing date, SD1: 26. Sept. 2013, SD2: 17. Oct. 2014, wheat cultivars: X: *Xenos*, C: *Capo*

by increasing biomass production through increased RUE. The result was earlier, but still too late, initiation of tillering and severely worsened (higher) simulated vs. observed fits of biomass, yield and leaf development (data not presented).

The simulations of leaf area index (LAI) (Figure 25) and leaf number matched the observations variably. *Xenos* simulations were slightly better predicted than *Capo*. For SD2X, LAI in autumn and early spring were simulated very precisely, while in mid May (at flowering) LAI was overestimated. The simulation of the leaf number on the main stem was very good (Figure 26). Observed phyllochron was 113.6 °Cd.

For SD4X, LAI simulation overestimated observations in late April, then underestimated them strongly in late May and slightly in mid June (flowering). The leaf number on the main stem was very well predicted. Observed phyllochron was 103.1 °Cd.

For SD1X and C, prediction of the final leaf number on the main stem was worst of all

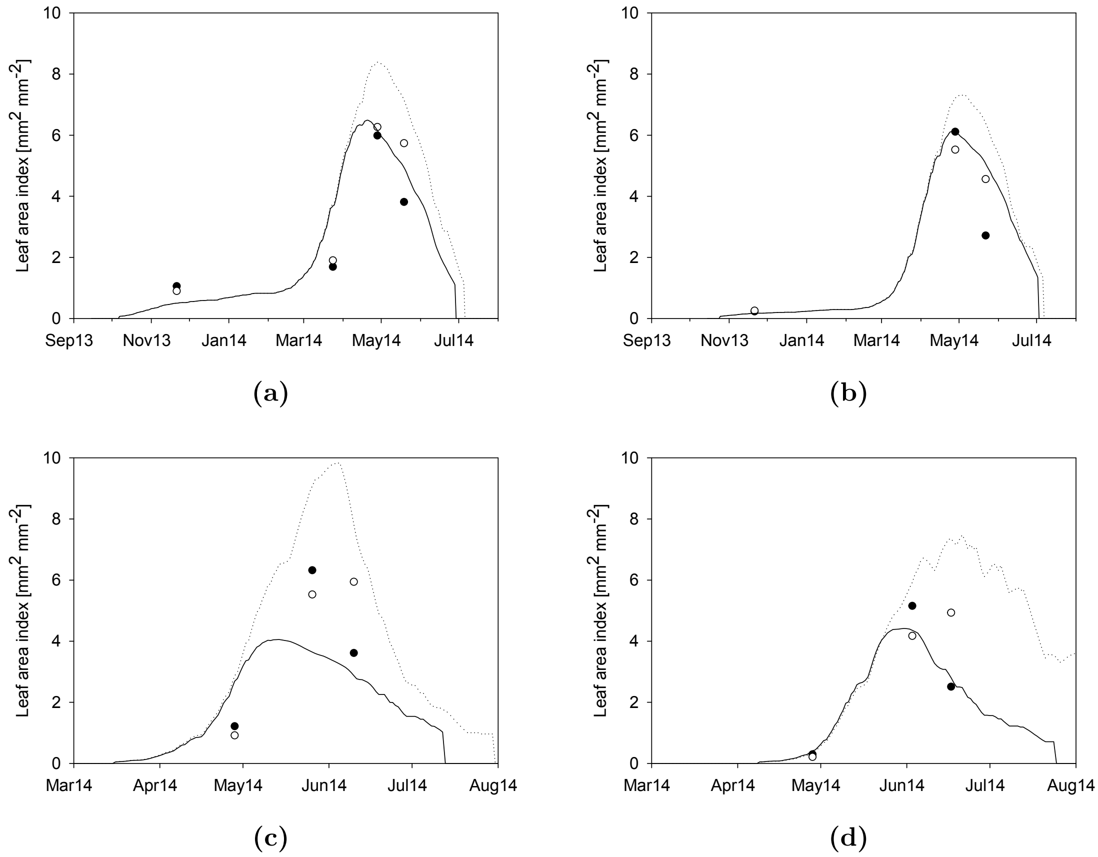

Figure 25 – Leaf area index simulations (lines) and observations (symbols) of (a) SD1, (b) SD2, (c) SD4, and (d) SD5. Closed symbols and full line: facultative wheat cultivar *Xenos*, open symbols and dotted line: winter wheat cultivar *Capo*. SD: Sowing date. SD1: Sep. 26, SD2: Oct. 17 in 2013, and SD4: Mar. 4, SD5: Apr. 1 in 2014.

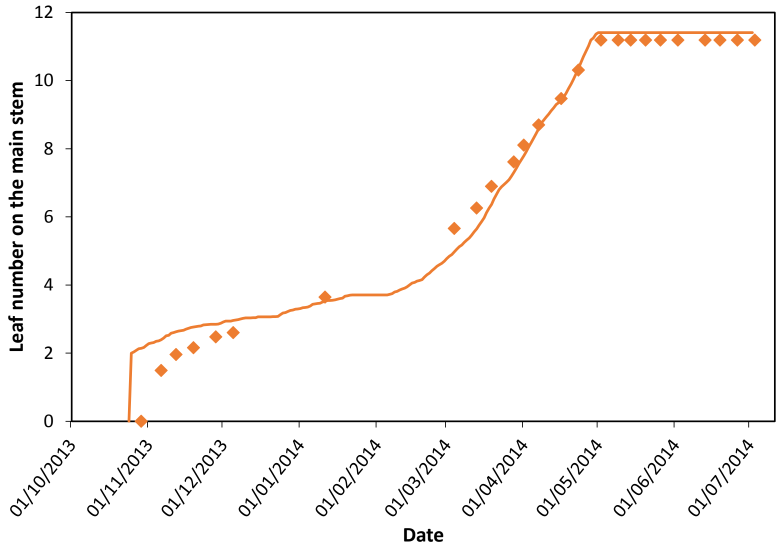

Figure 26 – Simulated (line) and observed (points) development of the leaf number on the main stem for sowing date 2 (17. October 2013), facultative wheat cultivar *Xenos*.

treatments (observed: *Xenos* 12 and *Capo* 12.6, simulated: *Xenos* 13.6 and *Capo* 15.3) when using APSIM's default value for phyllochron (95 °Cd). Observed phyllochrons were: *Xenos* 122 °Cd and *Capo* 125 °Cd. We set up another simulation, only changing APSIM's phyllochron to 122 °Cd. The leaf number simulation on the main stem was then very good for SD1. However, it worsened for all other simulations. Best overall results were achieved using the default phyllochron of 95 °Cd.

Overall prediction of biomass was very robust for *Xenos*, while *Capo* simulations matched observations variably well. SD1C & SD2C were underestimated while SD4C & SD5C were overestimated (Figure 27). In autumn, biomass of SD1 and SD2 was underestimated for both cultivars (Table 5).

Yield simulation was better for *Xenos* than for *Capo* (Figure 28). *Xenos* SD1 & SD4 and *Capo* SD2 & SD3 were predicted very exactly. However, SD4C was largely overestimated and SD5C failed to produce yield which was simulated correctly.

5.6 Comparison of Two Meteorological Datasets

The Raasdorf daily weather data (rainfall, global radiation, minimum and maximum temperatures) was used for the simulations. The data was displayed graphically in the GUI of APSIM and checked for errors visually as well as with the software TAMET (Wall 1977). No inconsistencies were found in the data.

Nevertheless, the comparisons between simulated and observed soil water contents

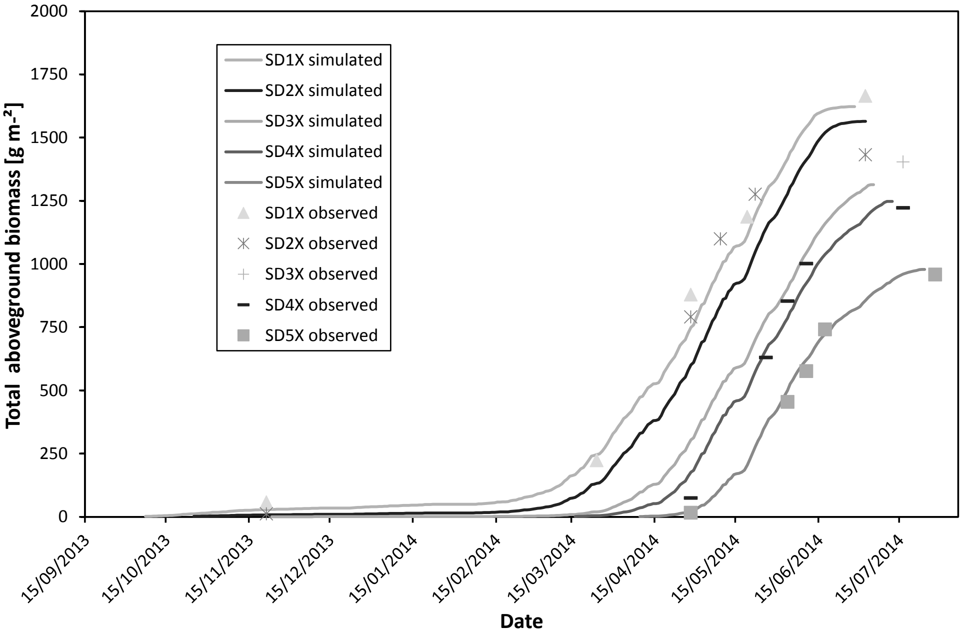

(a)

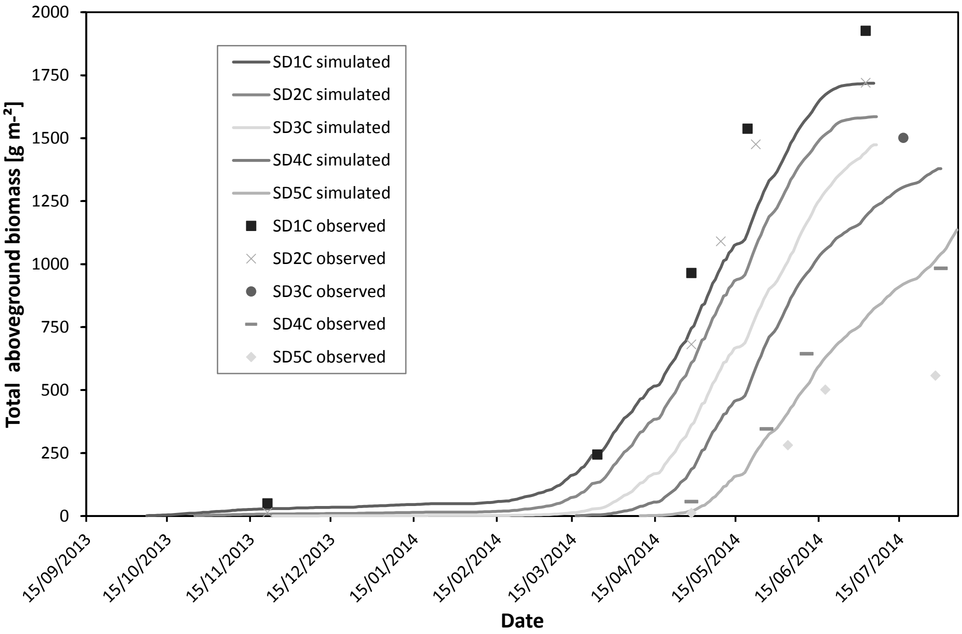

(b)

Figure 27 – Simulated (curves) versus observed (symbols) biomass development of (a) facultative wheat cultivar *Xenos* (X) and (b) winter wheat cultivar *Capo* (C). SD: sowing date (SD1: Sep. 26, SD2: Oct. 17, SD3: Nov. 7 in 2013, and SD4: Mar. 4, and SD5: Apr. 1 in 2014).

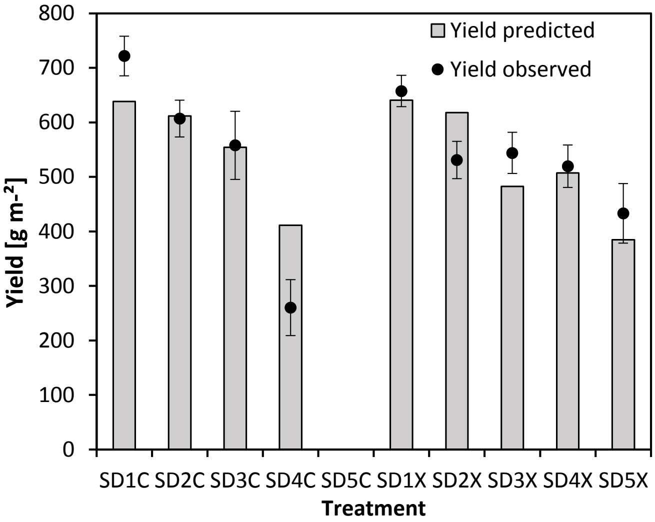

Figure 28 – Simulated (bars) and observed (symbols) grain yields. Standard error bars for observed values. X: facultative wheat cultivar *Xenos*, C: winter wheat cultivar *Capo*, SD: sowing date (SD1: Sep. 26, SD2: Oct. 17, SD3: Nov. 7 in 2013, and SD4: Mar. 4, and SD5: Apr. 1 in 2014).

identified potential errors in the Raasdorf precipitation data. For instance, peaks in the simulated soil water content in the top soil layers (caused by observed precipitations) which do not fit observed soil water data (e.g. Figure 20b around 15. April 2014) might be due to incorrect (i.e. too high) precipitation data. To investigate this, the weather data files in APSIM were modified (e.g. precipitation values set to zero) and the simulations were rerun. However, reducing the precipitation in this manner always resulted in worsening the matches between simulated and observed biomass and yield, and soil water content simulations hardly improved.

For further testing of the Raasdorf meteorological data it was compared to another station nearby (Groß-Enzersdorf, run by the Zentralanstalt für Meteorologie und Geodynamik [ZAMG]). Data from the ZAMG station showed differences to the Raasdorf data. The correlations were (R^2 in brackets): daily maximum temperature (0.976), daily minimum temperature (0.930), global radiation (0.958), and precipitation (0.628). Deviations of precipitation occurred mainly in April 2014 (Raasdorf: 69.4 mm, Groß-Enzersdorf: 126.4 mm) and May 2014 (Raasdorf: 67.2 mm, Groß-Enzersdorf: 104.9 mm). Daily minimum and maximum temperatures were generally higher in Groß-Enzersdorf. Global radiation was also higher in Groß-Enzersdorf, especially between March 2014 and harvest (total cumulated difference at 30. July: 308 MJ m^{-2}, Figure 9d).

We set up an identical simulation, only using the Groß-Enzersdorf weather data instead of Raasdorf. The simulated phenological development was faster, e.g. average anthesis of all treatments occurred 2.4 days earlier than observed (0.3 days earlier with

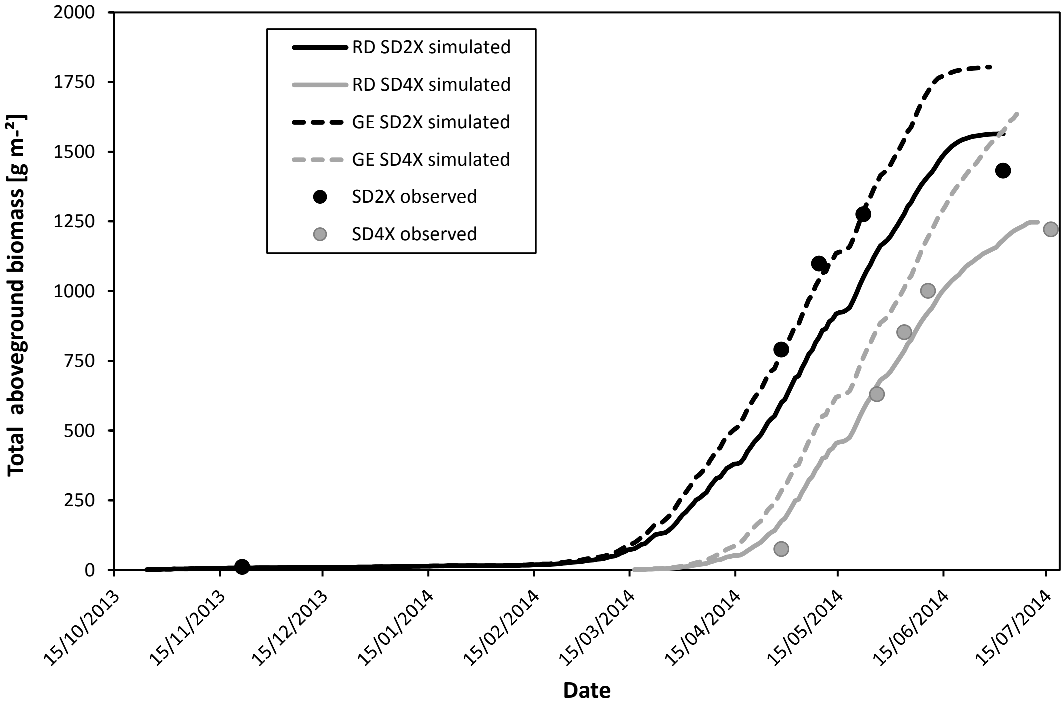

Figure 29 – Biomass for SD2X and SD4X, simulated (lines) with Raasdorf (RD) and Groß-Enzersdorf (GE) weather data, compared to observations (symbols). X: facultative wheat cultivar *Xenos*, C: winter wheat cultivar *Capo*, SD: sowing date (SD2: 17. October 2013, SD4: 4. March 2014).

Raasdorf data). Total biomass and yield were also higher for all treatments (Figure 29 and Figure 30) as well as LAI.

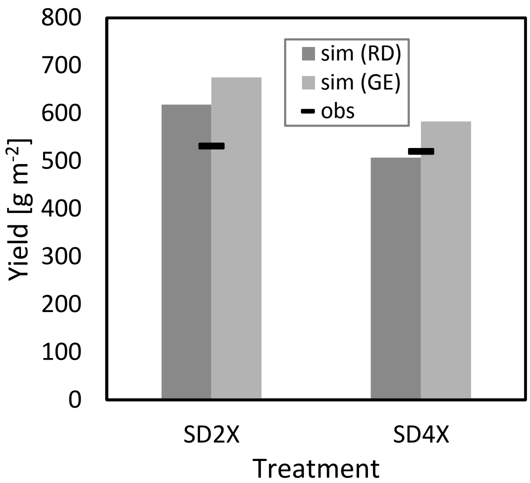

(a)

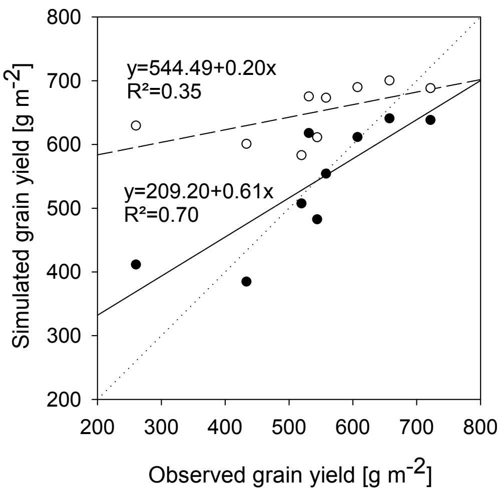

(b)

Figure 30 – (a) Simulated (sim, bars) compared to observed (obs, symbols) grain yield of SD2X and SD4X with Raasdorf (RD) and Groß-Enzersdorf (GE) weather data. X: facultative wheat cultivar *Xenos*, C: winter wheat cultivar *Capo*, SD: sowing date (SD2: 17. October 2013, SD4: 4. March 2014). (b) Simulated over observed grain yield of all treatments for RD (closed symbols and full line) and GE (open symbols and dashed line). Dotted: 1:1 line.

6 Discussion

6.1 Weather Condition

Compared to the long term average, the weather at Raasdorf was very dry in winter (Dec.-Mar.) and wet in spring and early summer (Apr.-Jul.) (Figure 8). The temperature (Figure 9a) was relatively high during a 4 weeks period (end Dec.-Jan.), followed by 10 days below average daily maximum temperatures but approximately average daily minimum temperatures. Most likely, persistent fog caused this low amplitude between minimum and maximum temperatures. The remaining season was characterized by average daily minimum temperatures and mainly above average daily maximum temperatures, with some below average depressions (Apr.-Jul.) accompanied by larger amounts of precipitation.

6.2 Phenology, Biomass and Yield

APSIM predicted emergence 3 to 26 days earlier than observed. Another study by Moeller et al. (2007) also found that APSIM places emergence too early in simulations. They stated that this earliness might partly be explained by the fact that the model simulates germination depending solely on soil moisture. However, APSIM includes other parameters for simulating emergence, such as temperature and sowing depth (Zheng et al. 2014). For SD3 and SD4 we assume that observed emergence was severely influenced by a soil crust (Figure 17) which is not implemented in APSIM. Especially in SD4 we found plants which were not able to penetrate the thick and compact soil surface layer and eventually died below ground. In addition, we suspect the low temperatures in combination with an uneven sowing depth to have caused a low emergence rate, particularly for SD3.

The initiation of tillering for the autumn sown treatments (SD1, SD2, and SD3) was simulated too late, while the spring sown treatments matched well (Figure 24). As described in section 2, APSIM simulates tillers indirectly by simulating an increasing number of leaves per increasing main stem node number on the single-stemmed plants (Zheng et al. 2014). However, this is just the potential leaf number. The actual leaf number is dependent on the relation of other factors which are not clearly documented (see Zheng et al. 2014, section 7.2). Nevertheless, the cause for the delay in tiller simulation initiation is very likely to be embedded in this relation. Since only the autumn sown treatments were affected, it appears possible that the problem was triggered by the long lasting low temperatures in late autumn and winter.

Simulated phenological development was faster, including earlier flowering, when using the precipitation-richer Groß-Enzersdorf weather data (Figure 9c) instead of Raasdorf. The impression that faster development is a result of more rainfall is deceiving. The data comparison shows that most of the additional rainfall at Groß-Enzersdorf occurred from late April 2014 on, only about two weeks before flowering of the first treatments and, therefore, too late to affect their date of flowering. Furthermore, a relatively large amount of precipitation during winter is missing at Groß-Enzersdorf compared to Raasdorf, thereby raising soil water content for Raasdorf significantly above Groß-Enzersdorf for about three months (e.g. for SD2X: Figure 31). As a result, Groß-Enzersdorf weather data led to lower soil water content than Raasdorf weather data for a major part at the beginning of the growing season. Especially the hastened anthesis at reduced water availability goes in accordance with real world expectations observed in other studies (McMaster and Wilhelm 2003; Moeller et al. 2007). However, this does not explain why the model simulated earlier anthesis since APSIM does not include dry stress in the prediction of phenology. Instead, increased global radiation (Figure 9b) at Groß-Enzersdorf has probably caused the simulated faster development.

The winter wheat cultivar *Capo* failed the transition into reproductive phase (Figure 24b) for the last sowing date (1. April 2014). This is clearly a consequence of the lack of vernalization. The model was able to accurately predict this behavior after adjusting the relevant parameter (`vern_sens`) in APSIM's *Wheat* XML file.

Mouse feeding and burrowing were persisting problems throughout the whole experiment. Furthermore, frequent rust fungus (*Puccinia striiformis*) infections were promoted by wet weather conditions (starting in late April) and sometimes enhanced by late fungicide applications. Neither mouse damage nor fungal infections were accounted for in the simulations due to the lack of appropriate sub-models in APSIM. Assuming that those pests and diseases reduced yield and biomass, the overestimation for SD1C would be reduced. In contrast, the underestimation of e.g. SD2X would further increase (Figure 28, Figure 27).

The observed wheat grain yields (autumn sown *Xenos* and *Capo*: $531\,\mathrm{g\,m^{-2}}$ to $722\,\mathrm{g\,m^{-2}}$, spring sown *Xenos*: 433 and $520\,\mathrm{g\,m^{-2}}$, Figure 28) were relatively high compared to other wheat experiments carried out in the same area. Neugschwandtner et al. (2015b) found $479\,\mathrm{g\,m^{-2}}$ for autumn-sown and $336\,\mathrm{g\,m^{-2}}$ for spring-sown *Xenos* wheat in a 2-year experiment and Neugschwandtner et al. (2015a) reported $365\,\mathrm{g\,m^{-2}}$ for autumn-sown *Capo* wheat in one year, and 130 to $623\,\mathrm{g\,m^{-2}}$ for different wheat cultivars in a long term experiment.

6.3 Canopy Development

LAI predictions were ambiguous (Figure 25). Similarly, other studies (Meinke et al. 1997; Asseng et al. 1998; Asseng et al. 2000) found poor LAI predictions (mainly overestimations) of the APSIM *Wheat* model.

Our results emphasize that APSIM's assumption of a cultivar independent constant phyllochron (95 °Cd) is a simplification that is roughly appropriate for standard sowing dates only. For SD2, SD3, and SD4X (ignoring SD1 since it was relatively early, and SD4 and SD5 since they were not sensible sowing dates for a winter wheat cultivar), average phyllochron was 97 °Cd which was close to APSIM's phyllochron. However, considering all (106.6 °Cd) or only the regionally most common (SD2, 118 °Cd) sowing dates of the experiment, observed phyllochrons exceeded the model's assumption. In addition, APSIM starts simulations with two initial leaves and modifies phyllochron: once for the spring sown treatments, twice for the autumn sown treatments. This resulted in effectively two phyllochrons for the autumn sown treatments: the first with a greater, the second with a smaller modified phyllochron (Figure 19a for SD2X). It seems that the modification of phyllochron (once or twice) aims at correcting the error of setting initial two leaves in order to correctly simulate the final leaf number. We found good prediction of the final leaf number for SD2, but poor prediction for e.g. SD1. Furthermore, the simulation of leaf number development was necessarily poor, specifically for the autumn sown treatments where the non-linear simulation graph (starting with intercept two) could never fit the linear observations (starting at one).

APSIM underestimated aboveground biomass of *Capo* SD1 and SD2, but overestimated SD4 and SD5. Observed phyllochrons (SD1C: 125, SD2C: 112, SD4C: 103, and SD5C: 130 °Cd) suggest a higher phyllochron than APSIM's default for *Capo*. The effects of an increased phyllochron on biomass simulation would be ambiguous. In short, the number of leaves would be reduced and, therefore, biomass as well. As a result, underestimation of *Capo* SD1 and SD2 would increase further, but overestimation of SD4 and SD5 would be reduced.

The observed differences in leaf orientation for the two contrasting wheat cultivars have potential implications on radiation interception. In APSIM, this difference is only partially ascertainable by modifying the light extinction coefficient (k). However, Falster and Westoby (2003) and other studies have shown that shallower leaf angles generally result in higher whole day radiation interception.

6.4 Soil Water

Calibration of the soil water content was a challenging task. Regarding the two datasets available (soil sampled and *Diviner* sensor measured), there was no continued trend showing which one of them was more precise. Within one treatment, the simulated trends often alternated which of the two datasets they were a better fit for, sometimes even between adjacent soil layers. Furthermore, observed trends of neighboring layers were sometimes offset greatly so that the simulated trends deviated significantly due to unsaturated flow. In those cases, an erroneous offset in the measurements was anticipated. Those decisions had to be made for every layer, in addition to comparing more than two layers, while inspecting the biomass simulations at the same time. Afterwards, the initial soil water content was adjusted, the simulations were run again and the output compared to observations. This process was repeated several times. Truly reliable soil water content and meteorological datasets for parameterization would make this calibration process unnecessary. Also, the achievement of correctly simulated biomass development is tightly bound to an accurate soil water content simulation.

We found two water related differences between observations and simulations which we could not clarify. One was the significantly lower observed soil water content in upper soil layers during the last months of the experiment, the other an observed dry stress of SD1 and SD2 in mid March which was not simulated by APSIM. Concerning the observed soil water content deviations, it is possible that inevitable errors through field conditions have distorted the *Diviner* measurements. For instance, mouse burrowing close to the PVC access tubes might have changed the soil bulk density within the measurement radius and therefore distorted (reduced) the measured soil water content by a rather constant value.

Another plausible explanation for the discrepancies in soil water content between observations and simulations in the upper soil layers, starting in April 2014 (Figure 20, Figure 21, Figure 31), is potentially erroneous precipitation data. In the simulation of SD2X, frequent rainfalls fill the 10 cm to 20 cm soil layer several times up to the drained upper limit, while the *Diviner* observation points fall steadily, showing no water content increase (except for 20. May 2014). In this period, thunderstorms occurred frequently, causing locally high precipitations in short time intervals. It is likely that during such thunderstorms the meteorological station at Raasdorf, although close (distance about 1 km) to the field experiment, received and measured higher amounts of precipitation than the field experiment. To investigate this, we modified the weather data (not provided) and set some precipitations at the end of April to zero (−51 % of total April precipitation). The soil water content simulation was improved partly, while simulated biomass and yield (particularly for SD1C and SD2C) decreased due to higher dry stress in June, reducing the match to the observations. The used cultivars *Xenos* and *Capo* might have a higher water use efficiency than anticipated in the model. However, water use efficiency is considered equal for all cultivars in APSIM's *Wheat* model.

Local thunderstorms, as described above, are the probable cause for differences between precipitation data of Raasdorf and Groß-Enzersdorf. For instance, in SD2X there is a clear observed (*Diviner*) soil water content increase in the 10 cm to 20 cm layer on 12. November 2013. This was simulated well with the Raasdorf weather data, but was

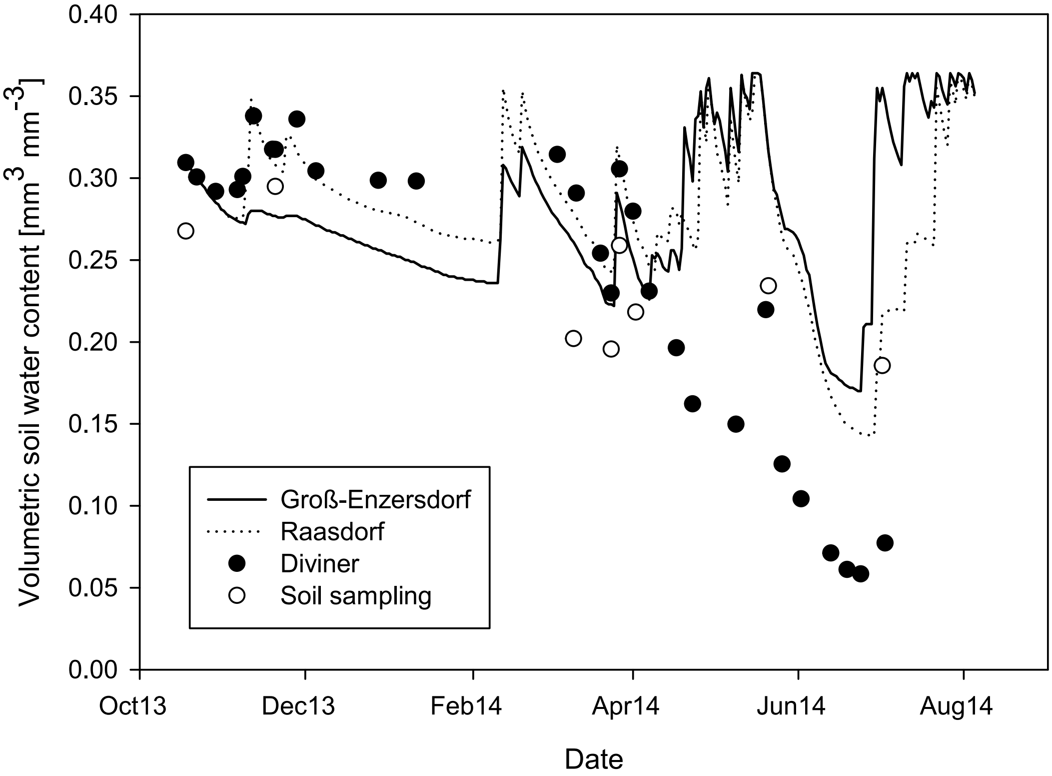

Figure 31 – Soil water content for sowing date 2 (17. October 2013) of wheat cultivar *Xenos*, soil layer 10 cm to 20 cm. The curves show simulation results for the two different weather datasets (Raasdorf and Groß-Enzersdorf). Closed symbols (*Diviner* sensor measurements) and open symbols (soil samples, gravimetric [converted to volumetric]) represent the observations.

almost missing with Groß-Enzersdorf data (Figure 31), thereby confirming the Raasdorf data.

We observed dry stress of SD1 and SD2 (and also in different neighboring cereal fields) in mid March which could not be reproduced in the simulations. We suspected exceedingly high rooting depths in early spring (e.g. over 1000 mm for SD1X simulated on 15 March 2014) to be the main reason. Consequently, we reduced APSIM's `root_depth_rate` for the phenological stages (Figure 3) occurring during winter (stage; reduced/default `root_depth_rate` [$\mathrm{mm\,d^{-1}}$]): 3; 5/30, 4; 15/30. This reduced the rooting depths significantly (SD1X: 620 mm, 15 March 2014). However, there was still no dry stress in the simulations, but the soil water content match to observations worsened. Therefore, we reverted to the default values. In other respects, local snow drifts during winter (not captured by APSIM) might have affected water supply to the plants to a limited extend which we did not investigate. However, the early sowing (particularly of SD1) in combination with the rather high sowing density (360 plants $\mathrm{m^{-2}}$) and the mild winter have led to a relatively dense and biomass-rich plant canopy in early spring. As a result, water demand was high at that time which has, in combination with the low winter precipitation, presumably caused the observed dry stress. Nevertheless, APSIM should be able to capture those processes.

Another factor which most likely affected soil water relations, but is not accounted for in APSIM, was wind. At the experimental site at Raasdorf, strong persistent winds were observed regularly by the local staff (average wind speed at Raasdorf from 1. Sept. 2013 to 31. Aug. 2014: 10.4 $\mathrm{km\,h^{-1}}$) and are known to be common. In addition, there was only one windbreak hedge nearby which had poor efficiency due to its parallel alignment to the prevailing wind direction (west). Wind could be at least part of the explanation for the soil water content deviations in the topmost soil layer, but seems rather unlikely to have a considerable impact on deeper layers or even explain the large deviations starting in April 2014.

Reliability of gravimetric and sensor (*Diviner*) determined soil water content was ambiguous. Gravimetric data was calculated from soil samples taken randomly across the plot, ideally. However, a true randomization in this context was not possible since physical access to the center of the plots would have included serious damage to the canopy, particularly considering the frequent occurrences of those measurements and the relatively small plot size. Therefore, samples were taken randomly at both ends of the plot, moving further to the center for the following samplings and leaving enough plot area undamaged for other samplings such as crop biomass. As a result, measurements might deviate significantly from reality. Additionally, despite all precautions, soil water might have got lost during transportation before weighing of fresh mass (e.g. due to condensation water on the inside of the plastic bags used to wrap the soil samples). Groves and Rose (2004) showed *Diviner's* capability to obtain highly significant soil water content estimates under laboratory conditions. Still, multiple sources of error, especially under field conditions, are possible. Most important of which are wet access tubes or a wet sensor head and the fact that there was only one access tube installed at the middle of each plot. Nevertheless, sensor measurements are certainly at least a good indicator for the soil water content trend, given their frequency. The agreement between large parts of simulated and observed (soil sampled and sensor measured) soil water content supports the assumption of good quality data, although some questions, as described above, remain unanswered.

6.5 Further Remarks

Although APSIM includes nitrogen dynamics (supply and demand) in its models, those were not included in our simulations.

The comparability of this experiment's results with farmer's practice is certainly limited. Besides the issues due to the small plot size (e.g. border effects), only one (SD2 on 17. Oct. 2013) of the five sowing dates matched the local farmer's typical time frame for winter wheat. Spring sown wheat (except durum wheat) is rather uncommon, and spring sown winter wheat (treatments SD4C and SD5C) is apparently of scientific interest only.

Besides all scientific attempts to find explanations for the prediction's departures from reality, we need to bear in mind that the model's input data (e.g. for soil characteristics) is given as point data for the whole experiment and thus cannot capture the indefinitely fine resolution of variation in the real world (e.g. soil properties within sites) (Palosuo et al. 2011). Models cannot and do not claim the ability to perfectly represent reality. Therefore, a certain prediction error needs to be anticipated among the model's simplifications.

7 Conclusion

The comparisons of simulated and observed data show that APSIM is capable of capturing the cultivar-specific differences of the winter and the facultative wheat cultivar concerning phenology, biomass, and yield in the chosen environment. The model parameters determining the different phenological developments are the factors for photoperiod and vernalization. These parameters need to be calibrated by trial and error for each cultivar.

Despite its overall prediction capability in this study, there were significant differences between the simulations and observations. We found three factors to be the main causes: field dataset inconsistencies, model omissions, and model internal biases. The field dataset (plant, soil, and meteorological observations) contributed to the discrepancies mainly through unreliable soil water content and precipitation data. Those led to unsure soil water content simulations, which have a vast impact on many physiological processes and, therefore, on biomass production. A reliable parameterization dataset is crucial to ensure accurate predictions of crop grain yield and biomass. Model omissions summarize the model's inability to simulate important real world processes such as pests and diseases which influence the crop's biomass production and phenological development. Model internal biases are assumptions within the model which simply fail to correctly reflect reality. We suspect such errors to be the reasons for the late simulated initiation of tillering for the autumn sown treatments. Also, leaf development estimations were poor, probably caused by APSIM's allegedly wrong assumption of a cultivar-independent phyllochron which the model modified non-linearly for autumn sowing dates. From our experiment we conclude that phyllochron is constant and cultivar-specific.

The validity of a one year experiment is certainly limited. Therefore, we suggest further studies to investigate our conclusions.

8 References

APSIM Documentation: SoilWat (2015). URL: https://www.apsim.info/Documentation/Model,CropandSoil/SoilModulesDocumentation/SoilWat.aspx (visited on 11/14/2015).

APSIM & The APSIM Initiative (2014). URL: http://www.apsim.info/Portals/0/Documentation/APSIM%20Overview.pptx (visited on 11/11/2014).

Asseng, S., Ewert, F., Rosenzweig, C., Jones, J. W., Hatfield, J. L., Ruane, A. C., Boote, K. J., Thorburn, P. J., Rotter, R. P., Cammarano, D., Brisson, N., Basso, B., Martre, P., Aggarwal, P. K., Angulo, C., Bertuzzi, P., Biernath, C., Challinor, A. J., Doltra, J., Gayler, S., Goldberg, R., Grant, R., Heng, L., Hooker, J., Hunt, L. A., Ingwersen, J., Izaurralde, R. C., Kersebaum, K. C., Muller, C., Naresh Kumar, S., Nendel, C., O/'Leary, G., Olesen, J. E., Osborne, T. M., Palosuo, T., Priesack, E., Ripoche, D., Semenov, M. A., Shcherbak, I., Steduto, P., Stockle, C., Stratonovitch, P., Streck, T., Supit, I., Tao, F., Travasso, M., Waha, K., Wallach, D., White, J. W., Williams, J. R., and Wolf, J. (2013). "Uncertainty in simulating wheat yields under climate change." In: *Nature Clim. Change* 3.9, pp. 827–832.

Asseng, S., Keating, B., Fillery, I., Gregory, P., Bowden, J., Turner, N., Palta, J., and Abrecht, D. (1998). "Performance of the APSIM-wheat model in Western Australia." In: *Field Crops Research* 57.2, pp. 163–179.

Asseng, S., Keulen, H. van, and Stol, W. (2000). "Performance and application of the APSIM Nwheat model in the Netherlands." In: *European Journal of Agronomy* 12.1, pp. 37–54.

Asseng, S., Foster, I., and Turner, N. C. (2011). "The impact of temperature variability on wheat yields." In: *Global Change Biology* 17.2, pp. 997–1012.

Bassu, S., Brisson, N., Durand, J.-L., Boote, K., Lizaso, J., Jones, J. W., Rosenzweig, C., Ruane, A. C., Adam, M., Baron, C., Basso, B., Biernath, C., Boogaard, H., Conijn, S., Corbeels, M., Deryng, D., De Sanctis, G., Gayler, S., Grassini, P., Hatfield, J., Hoek, S., Izaurralde, C., Jongschaap, R., Kemanian, A. R., Kersebaum, K. C., Kim, S.-H., Kumar, N. S., Makowski, D., Müller, C., Nendel, C., Priesack, E., Pravia, M. V., Sau, F., Shcherbak, I., Tao, F., Teixeira, E., Timlin, D., and Waha, K. (2014). "How do various maize crop models vary in their responses to climate change factors?" In: *Global Change Biology* 20.7, pp. 2301–2320.

Boote, K. J., Jones, J. W., and Pickering, N. B. (1996). "Potential Uses and Limitations of Crop Models." In: *Agronomy Journal* 88.5, pp. 704–716.

Brown, H. E., Huth, N. I., Holzworth, D. P., Teixeira, E. I., Zyskowski, R. F., Hargreaves, J. N. G., and Moot, D. J. (2014). "Plant Modelling Framework: Software for building and running crop models on the APSIM platform." In: *Environmental Modelling & Software* 62, pp. 385–398.

Eck, C., Garcke, H., and Knabner, P. (2011). *Mathematische Modellierung*. Springer-Lehrbuch. Berlin, Heidelberg: Springer Berlin Heidelberg.

Eitzinger, J., Thaler, S., Schmid, E., Strauss, F., Ferrise, R., Moriondo, M., Bindi, M., Palosuo, T., Rötter, R., and Kersebaum, K. C. (2013). "Sensitivities of crop models to extreme weather conditions during flowering period demonstrated for maize and winter wheat in Austria." In: *The Journal of Agricultural Science* 151.6, pp. 813–835.

Falster, D. S. and Westoby, M. (2003). "Leaf size and angle vary widely across species: what consequences for light interception?" In: *New Phytologist* 158.3, pp. 509–525.

Google Maps (2016). URL: https://www.google.at/maps/@48.2243181,16.5116611,12z (visited on 01/16/2016).

Groves, S. J. and Rose, S. C. (2004). "Calibration equations for Diviner 2000 capacitance measurements of volumetric soil water content of six soils." In: *Soil Use and Management* 20.1, pp. 96–97.

Hammer, G. L., Dong, Z., McLean, G., Doherty, A., Messina, C., Schussler, J., Zinselmeier, C., Paszkiewicz, S., and Cooper, M. (2009). "Can changes in canopy and/or root system architecture explain historical maize yield trends in the US corn belt?" In: *Crop Science* 49.1, pp. 299–312.

Holzworth, D. P., Huth, N. I., and deVoil, P. G. (2011). "Simple software processes and tests improve the reliability and usefulness of a model." In: *Environmental Modelling & Software* 26.4, pp. 510–516.

Holzworth, D. P., Huth, N. I., deVoil, P. G., Zurcher, E. J., Herrmann, N. I., McLean, G., Chenu, K., Oosterom, E. J. van, Snow, V., Murphy, C., Moore, A. D., Brown, H., Whish, J. P., Verrall, S., Fainges, J., Bell, L. W., Peake, A. S., Poulton, P. L., Hochman, Z., Thorburn, P. J., Gaydon, D. S., Dalgliesh, N. P., Rodriguez, D., Cox, H., Chapman, S., Doherty, A., Teixeira, E., Sharp, J., Cichota, R., Vogeler, I., Li, F. Y., Wang, E., Hammer, G. L., Robertson, M. J., Dimes, J. P., Whitbread, A. M., Hunt, J., Rees, H. van, McClelland, T., Carberry, P. S., Hargreaves, J. N., MacLeod, N., McDonald, C., Harsdorf, J., Wedgwood, S., and Keating, B. A. (2014). "APSIM – Evolution towards a new generation of agricultural systems simulation." In: *Environmental Modelling & Software* 62, pp. 327–350.

Huth, N. I., Thorburn, P. J., Radford, B. J., and Thornton, C. M. (2010). "Impacts of fertilisers and legumes on N 2 O and CO 2 emissions from soils in subtropical agricultural systems: a simulation study." In: *Agriculture, Ecosystems & Environment* 136.3, pp. 351–357.

Keating, B., Carberry, P., Hammer, G., Probert, M., Robertson, M., Holzworth, D., Huth, N., Hargreaves, J., Meinke, H., Hochman, Z., McLean, G., Verburg, K., Snow, V., Dimes, J., Silburn, M., Wang, E., Brown, S., Bristow, K., Asseng, S., Chapman, S., McCown, R., Freebairn, D., and Smith, C. (2003). "An overview of APSIM, a model designed for farming systems simulation." In: *European Journal of Agronomy* 18.3, pp. 267–288.

Littell, R. C., Freund, R. J., and Spector, P. C. (1991). "SAS system for linear models." In: *Cary, NC: SAS Institute Inc.*

Littleboy, M., Silburn, D. M., Freebairn, D. M., Woodruff, D. R., and Hammer, G. L. (1989). "PERFECT - A computer simulation model of Productivity Erosion Runoff Functions to Evaluate Conservation Techniques." In: *Bulletin-Queensland Department of Primary Industries (Australia).*

Manschadi, A. M., Christopher, J., and Hammer, G. L. (2006). "The role of root architectural traits in adaptation of wheat to water-limited environments." In: *Functional Plant Biology* 33.9, pp. 823–837.

Manschadi, A. M., Kaul, H.-P., Vollmann, J., Eitzinger, J., and Wenzel, W. (2014). "Developing phosphorus-efficient crop varieties—An interdisciplinary research framework." In: *Field Crops Research* 162, pp. 87–98.

McCown, R. L. and Williams, J. (1989). "AUSIM: a cropping systems model for operational research." In: *Proceedings of Eighth Biennial Conference on Modelling and Simulation, Australian National University*, pp. 25–27.

McMaster, G. S. and Wilhelm, W. W. (2003). "Phenological responses of wheat and barley to water and temperature: improving simulation models." In: *The Journal of Agricultural Science* 141.2, pp. 129–147.

Meinke, H., L. Hammer, G., Keulen, H. van, Rabbinge, R., and Keating, B. A. (1997). "Improving wheat simulation capabilities in Australia from a cropping systems perspective: water and nitrogen effects on spring wheat in a semi-arid environment." In: *European Journal of Agronomy* 7.1, pp. 75–88.

Meinke, H. and Stone, R. C. (2005). "Seasonal and inter-annual climate forecasting: the new tool for increasing preparedness to climate variability and change in agricultural planning and operations." In: *Climatic change* 70.1, pp. 221–253.

Moeller, C., Pala, M., Manschadi, A. M., Meinke, H., and Sauerborn, J. (2007). "Assessing the sustainability of wheat-based cropping systems using APSIM: model parameterisation and evaluation." In: *Australian Journal of Agricultural Research* 58.1, p. 75.

Monteith, J. L. (1996). "The Quest for Balance in Crop Modeling." In: *Agronomy Journal* 88.5, p. 695.

Neugschwandtner, R. W., Kaul, H. P., Liebhard, P., and Wagentristl, H. (2015a). "Winter wheat yields in a long-term tillage experiment under Pannonian climate conditions." In: *Plant Soil and Environment* 61.4, pp. 145–150.

Neugschwandtner, R. W., Böhm, K., Hall, R. M., and Kaul, H.-P. (2015b). "Development, growth, and nitrogen use of autumn- and spring-sown facultative wheat." In: *Acta Agriculturae Scandinavica, Section B—Soil & Plant Science* 65.1, pp. 6–13.

Neugschwandtner, R. W., Liebhard, P., Kaul, H.-P., and Wagentristl, H. (2014). "Soil chemical properties as affected by tillage and crop rotation in a long-term field experiment." In: *Plant, soil and environment* 60.2, pp. 57–62.

Palosuo, T., Kersebaum, K. C., Angulo, C., Hlavinka, P., Moriondo, M., Olesen, J. E., Patil, R. H., Ruget, F., Rumbaur, C., Takáč, J., Trnka, M., Bindi, M., Çaldağ, B., Ewert, F., Ferrise, R., Mirschel, W., Şaylan, L., Šiška, B., and Rötter, R. (2011). "Simulation of winter wheat yield and its variability in different climates of Europe: A comparison of eight crop growth models." In: *European Journal of Agronomy* 35.3, pp. 103–114.

Passioura, J. B. (1996). "Simulation Models: Science, Snake Oil, Education, or Engineering?" In: *Agronomy Journal* 88.5, p. 690.

Probert, M., Dimes, J., Keating, B., Dalal, R., and Strong, W. (1998). "APSIM's water and nitrogen modules and simulation of the dynamics of water and nitrogen in fallow systems." In: *Agricultural Systems* 56.1, pp. 1–28.

Reyenga, P., Howden, S., Meinke, H., and McKeon, G. (1999). "Modelling global change impacts on wheat cropping in south-east Queensland, Australia." In: *Environmental Modelling and Software with Environment Data News* 14.4, pp. 297–306.

Ritchie, J. T. and Otter-Nacke, S. (1985). "Description and performance of CERES-Wheat: a user-oriented wheat yield model." In: *USDA-ARS* 38, pp. 159–175.

Rötter, R. P., Carter, T. R., Olesen, J. E., and Porter, J. R. (2011). "Crop-climate models need an overhaul." In: *Nature Climate Change* 1.4, pp. 175–177.

Sinclair, T. R. (1986). "Water and nitrogen limitations in soybean grain production I. Model development." In: *Field Crops Research* 15.2, pp. 125–141.

Sinclair, T. R. and Seligman, N. G. (1996). "Crop Modeling: From Infancy to Maturity." In: *Agronomy Journal* 88.5, p. 698.

Soltani, A. and Sinclair, T. R., eds. (2012). *Modeling physiology of crop development, growth and yield*. Wallingford: CABI.

Soltani, A. and Sinclair, T. R. (2015). "A comparison of four wheat models with respect to robustness and transparency: Simulation in a temperate, sub-humid environment." In: *Field Crops Research* 175, pp. 37–46.

Verburg, K. (1996). *Methodology in soil-water-solute balance modelling: An objective comparison of the SoilWat, SALUS, and SWIMv2 models - s-dr-131.pdf*. Divisional Report 131. Australia: CSIRO, p. 95.

Wall, B. (1977). *TAMET: Computer program for processing meteorological data*. CSIRO Australia. Division of Tropical Crops and Pastures. Tropical Agronomy Technical Memorandum, pp. 4, 13.

Wessely, G. (2006). "Wiener Becken." In: *Geologie der österreichischen Bundesländer, Niederösterreich*. Vienna: Geologische Bundesanstalt (Geological Survey).

Yang, X., Asseng, S., Wong, M. T. F., Yu, Q., Li, J., and Liu, E. (2013). "Quantifying the interactive impacts of global dimming and warming on wheat yield and water use in China." In: *Agricultural and forest meteorology* 182, pp. 342–351.

Yang, Y., Yang, Y., Han, S., Macadam, I., and Li Liu, D. (2014). "Prediction of cotton yield and water demand under climate change and future adaptation measures." In: *Agricultural Water Management* 144, pp. 42–53.

Zadoks, J. C., Chang, T. T., and Konzak, C. F. (1974). "A decimal code for the growth stages of cereals." In: *Weed Research* 14.6, pp. 415–421.

Zhao, G., Bryan, B. A., and Song, X. (2014). "Sensitivity and uncertainty analysis of the APSIM-wheat model: Interactions between cultivar, environmental, and management parameters." In: *Ecological Modelling* 279, pp. 1–11.

Zheng, B., Chenu, K., Doherty, A., and Chapman, S. (2014). *The APSIM-Wheat Module (7.5 R3008)*. URL: https://www.apsim.info/Portals/0/Documentation/Crops/WheatDocumentation.pdf (visited on 09/10/2015).

9 List of Figures

10 List of Tables

11 Appendix

Table 6 – Various settings and parameters used in the APSIM simulations. Unless explicitly noted otherwise, the values were applied for all treatments.

Description	Value	Unit
Clock		
SD1	15.09.2013-05.08.2014	
SD2	15.10.2013-05.08.2014	
SD3, SD4, SD5	03.11.2013-05.08.2014	
Surface organic matter		
Organic matter pool name	barley	
Organic matter type	barley	
Initial surface residue	1000	$kg\,ha^{-1}$
C:N ratio of initial residue	80	
Fraction of residue standing	0	
Manager folder		
Sowing Dates		
SD1	26-sep	
SD2	17-oct	
SD3	7-nov	
SD4	4-mar	
SD5	1-apr	
Sowing Parameters		
Name of crop to sow (all SD)	wheat	
Sowing density SD1X	340	$plants\,m^{-2}$
Sowing density SD2X	360	$plants\,m^{-2}$
Sowing density SD3X	82	$plants\,m^{-2}$
Sowing density SD4X	243	$plants\,m^{-2}$
Sowing density SD5X	258	$plants\,m^{-2}$
Sowing density SD1C	340	$plants\,m^{-2}$
Sowing density SD2C	366	$plants\,m^{-2}$
Sowing density SD3C	128	$plants\,m^{-2}$
Sowing density SD4C	261	$plants\,m^{-2}$

Table 6 Continued: Various settings and parameters used in the APSIM simulations.

Description	Value	Unit
Sowing density SD5C	228	plants m^{-2}
Fertilise on a fixed date		
Fertiliser date 1 (all SD)	11-mar	
Fertiliser date 2 (all SD)	10-apr	
Don't add if N in top 2 layers exceeds	1000	kg ha^{-1}
Module used	fertiliser	
Amount	60	kg ha^{-1}
Fertiliser type	NH4NO3	
Irrigate on date		
Each year	yes	
Date	26-mar-2014	
Amount	25	mm
Irrigation efficiency	0.75	
Harvesting rule		
Name of crop	wheat	
Reset water on date		
Date of reset SD1	26-sep	
Date of reset SD2	17-oct	
Date of reset SD3	7-nov	
Date of reset SD4	4-mar	
Date of reset SD5	1-apr	
Raasdorf soil		
SoilWater (see also Table 7)		
Summer Cona	5	
Summer U	6	
Summer Date	1-Apr	
Winter Cona	3.5	
Winter U	6	
Winter Date	1-Nov	
Diffusivity Constant	40	
Diffusivity Slope	16	
Soil albedo	0.13	
Bare soil runoff curve number	73	
Max. reduction in curve number due to cover	20	
Cover for max curve number reduction	0.8	
SWCON (all layers)	0.300	

Table 6 Continued: Various settings and parameters used in the APSIM simulations.

Description	Value	Unit
SoilOrganicMatter (see also Table 7)		
Root C:N ratio	40	
Root Weight	200	kg ha^{-1}
Soil C:N ratio	15.5	
Erosion enrichment coefficient A	7.4	
Erosion enrichment coefficient B	0.2	
Wheat XML-file changes		
Cultivar specific		
`vern_sens` (X/C)	1.5, 5.0	
`photop_sens` (X/C)	4.6, 4.9	
`tt_end_of_juvenile` (X/C)	380, 380	°Cd
`tt_floral_initiation` (X/C)	520, 520	°Cd
General		
`initial_root_depth`	50	mm

SD: sowing date (SD1: Sep. 26, SD2: Oct. 17, SD3: Nov. 7 in 2013, and SD4: Mar. 4, and SD5: Apr. 1 in 2014), X: facultative wheat cultivar *Xenos*, C: winter wheat cultivar *Capo*.

Table 7 – Soil-related parameters used in the APSIM simulation component "Water". The values were applied for all treatments.

Depth [cm]	BD [g cm^{-3}]	AirDry	LL15	DUL [mm mm^{-1}]	SAT	Wheat LL	Wheat KL [d^{-1}]	Wheat XF (0-1)
0-10	1.203	0.100	0.130	0.300	0.315	0.130	0.10	1.0
10-20	1.280	0.100	0.130	0.350	0.370	0.130	0.10	1.0
20-30	1.270	0.110	0.110	0.350	0.370	0.110	0.08	1.0
30-40	1.270	0.090	0.090	0.350	0.370	0.090	0.08	1.0
40-50	1.200	0.070	0.070	0.300	0.315	0.070	0.05	1.0
50-60	1.220	0.050	0.050	0.300	0.315	0.050	0.05	1.0
60-70	1.250	0.050	0.050	0.280	0.294	0.050	0.05	1.0
70-80	1.270	0.050	0.050	0.280	0.294	0.050	0.05	1.0
80-90	1.330	0.050	0.050	0.280	0.294	0.050	0.04	1.0
90-100	1.330	0.050	0.050	0.270	0.283	0.050	0.03	1.0
100-110	1.330	0.050	0.050	0.270	0.283	0.050	0.03	1.0
110-120	1.330	0.050	0.050	0.250	0.263	0.050	0.03	1.0

Table 8 – Soil-related parameters used in the APSIM simulation components "SoilOrganicMatter" and "Analysis". The values were applied for all treatments.

Depth [cm]	OC Total %	FBiom (0-1)	FInert (0-1)	EC (1:5 dS/m)	pH (1:5 water)
0-10	2.155	0.040	0.370	0.200	8.400
10-20	2.145	0.035	0.370	0.225	8.600
20-30	2.135	0.030	0.370	0.250	8.800
30-40	1.550	0.030	0.520	0.280	8.900
40-50	1.550	0.030	0.520	0.310	9.000
50-60	1.550	0.030	0.520	0.330	9.100
60-70	0.897	0.020	0.890	0.350	9.100
70-80	0.897	0.020	0.890	0.370	9.150
80-90	0.897	0.020	0.890	0.400	9.200
90-100	0.897	0.020	0.950	0.450	9.200
100-110	0.897	0.020	0.950	0.510	9.200
110-120	0.897	0.020	0.950	0.590	9.200

Table 9 – Soil-related parameters used in the APSIM simulation component "Soil sample".

	Xenos		*Capo*	
Depth	NO3	SW	NO3	SW
		SD1		
0-10	9.200	0.210	9.200	0.230
10-20	19.700	0.290	19.700	0.260
20-30	30.200	0.320	30.200	0.270
30-40	25.600	0.300	25.600	0.290
40-50	15.600	0.220	15.600	0.250
50-60	5.500	0.200	5.500	0.220
60-70	1.900	0.200	1.900	0.220
70-80	2.700	0.200	2.700	0.210
80-90	3.500	0.200	3.500	0.200
90-100	4.800	0.170	4.800	0.170
100-110	4.400	0.130	4.400	0.150
110-120	4.100	0.130	4.100	0.130
		SD2		
0-10	9.200	0.250	9.200	0.230
10-20	19.700	0.310	19.700	0.300
20-30	30.200	0.340	30.200	0.270
30-40	25.600	0.260	25.600	0.250
40-50	15.600	0.230	15.600	0.230
50-60	5.500	0.200	5.500	0.200
60-70	1.900	0.180	1.900	0.180
70-80	2.700	0.180	2.700	0.180
80-90	3.500	0.220	3.500	0.200
90-100	4.800	0.220	4.800	0.200
100-110	4.400	0.200	4.400	0.170
110-120	4.100	0.130	4.100	0.130
		SD3		
0-10	13.400	0.250	19.300	0.250
10-20	18.500	0.240	32.300	0.300
20-30	40.600	0.280	28.500	0.290
30-40	42.700	0.280	34.500	0.270
40-50	39.900	0.250	24.700	0.250
50-60	17.900	0.210	17.000	0.230

Table 9 Continued: Soil-related parameters used in the APSIM simulation component "Soil sample".

	Xenos		*Capo*	
Depth	NO3	SW	NO3	SW
60-70	10.700	0.210	8.300	0.200
70-80	4.800	0.210	6.600	0.200
80-90	3.400	0.220	8.000	0.200
90-100	6.100	0.170	9.100	0.200
100-110	6.800	0.150	10.400	0.200
110-120	4.700	0.150	9.400	0.180
		SD4		
0-10	13.400	0.290	19.300	0.250
10-20	18.500	0.280	32.300	0.270
20-30	40.600	0.330	28.500	0.250
30-40	42.700	0.280	34.500	0.250
40-50	39.900	0.250	24.700	0.210
50-60	17.900	0.230	17.000	0.170
60-70	10.700	0.200	8.300	0.140
70-80	4.800	0.150	6.600	0.130
80-90	3.400	0.150	8.000	0.200
90-100	6.100	0.150	9.100	0.200
100-110	6.800	0.140	10.400	0.160
110-120	4.700	0.130	9.400	0.160
		SD5		
0-10	13.400	0.200	19.300	0.230
10-20	18.500	0.260	32.300	0.270
20-30	40.600	0.260	28.500	0.240
30-40	42.700	0.250	34.500	0.250
40-50	39.900	0.240	24.700	0.200
50-60	17.900	0.210	17.000	0.170
60-70	10.700	0.200	8.300	0.170
70-80	4.800	0.150	6.600	0.200
80-90	3.400	0.120	8.000	0.180
90-100	6.100	0.110	9.100	0.150
100-110	6.800	0.110	10.400	0.150
110-120	4.700	0.130	9.400	0.130

(a) 11. January 2014

(b) 28. March 2014

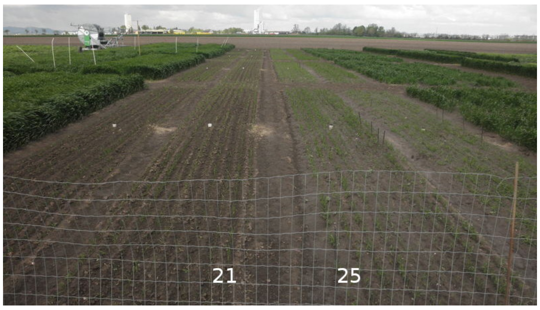

(c) 16. April 2014

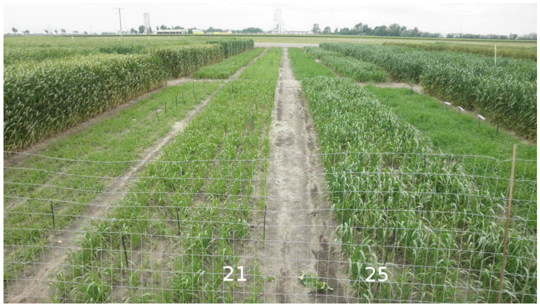

(d) 14. May 2014

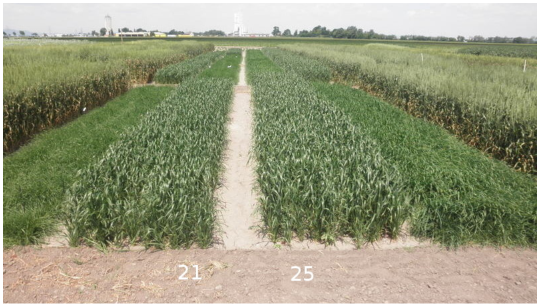

(e) 2. June 2014

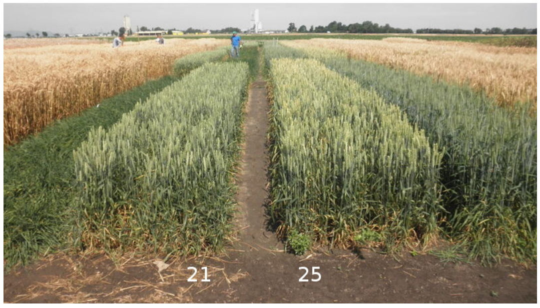

(f) 2. July 2014

Figure 32 – The field experiment at Raasdorf at different dates. Pictures were taken from approximately the same position (between SD5 (plot 21) and SD4 (plot 25), facing NW, see Figure 7), showing the sowing dates (SD) from left to right (SD1, SD2, SD5, SD4, SD3) and the replications from front to back (1-4).

(a) 18. October 2013

(b) 11. January 2014

(c) 1. April 2014

(d) 2. May 2014

(e) 2. June 2014

(f) 2. July 2014

Figure 33 – *Xenos* plants of plot 6 (sown on 26. September 2013) at different dates throughout the experiment.

(a) 18. October 2013

(b) 11. January 2014

(c) 1. April 2014

(d) 2. May 2014

(e) 2. June 2014

(f) 2. July 2014

Figure 34 – *Capo* plants of plot 7 (sown on 26. September 2013) at different dates throughout the experiment.

(a) 29. October 2013

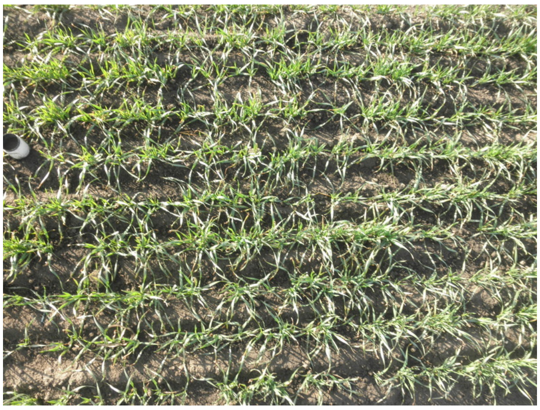

(b) 11. January 2014

(c) 1. April 2014

(d) 2. May 2014

(e) 2. June 2014

(f) 2. July 2014

Figure 35 – *Xenos* plants of plot 11 (sown on 17. October 2013) at different dates throughout the experiment.

(a) 29. October 2013

(b) 11. January 2014

(c) 1. April 2014

(d) 2. May 2014

(e) 2. June 2014

(f) 2. July 2014

Figure 36 – *Capo* plants of plot 15 (sown on 17. October 2013) at different dates throughout the experiment.

(a) 19. December 2013

(b) 11. January 2014

(c) 1. April 2014

(d) 2. May 2014

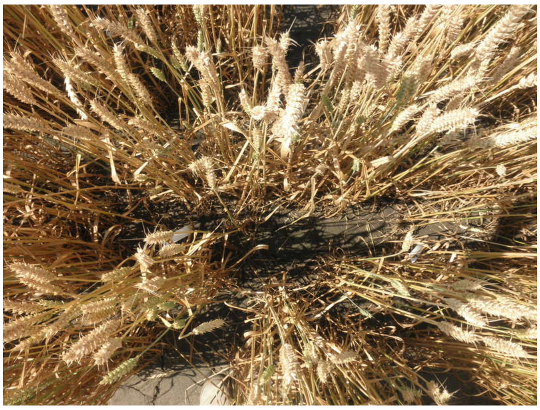

(e) 2. June 2014

(f) 2. July 2014

Figure 37 – *Xenos* plants of plot 36 (sown on 7. November 2013) at different dates throughout the experiment.

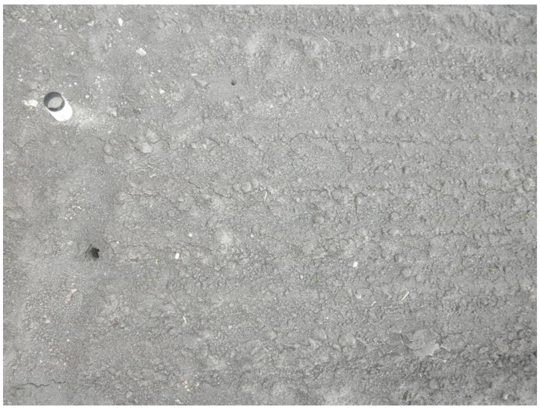

(a) 19. December 2013

(b) 11. January 2014

(c) 1. April 2014

(d) 2. May 2014

(e) 2. June 2014

(f) 2. July 2014

Figure 38 – *Capo* plants of plot 38 (sown on 7. November 2013) at different dates throughout the experiment.

(a) 1. April 2014

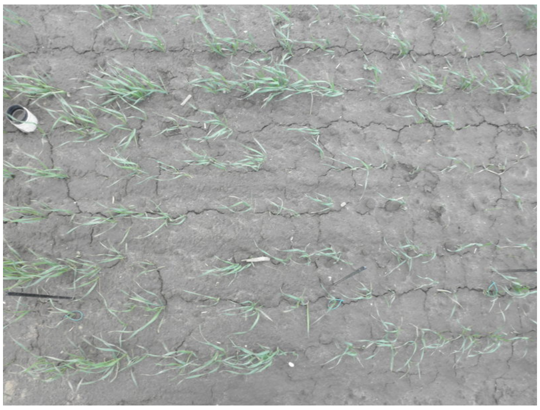

(b) 16. April 2014

(c) 2. May 2014

(d) 2. June 2014

(e) 2. July 2014

(f) 15. July 2014

Figure 39 – *Xenos* plants of plot 30 (sown on 4. March 2014) at different dates throughout the experiment.

(a) 1. April 2014

(b) 16. April 2014

(c) 2. May 2014

(d) 2. June 2014

(e) 2. July 2014

(f) 15. July 2014

Figure 40 – *Capo* plants of plot 28 (sown on 4. March 2014) at different dates throughout the experiment.

(a) 2. May 2014

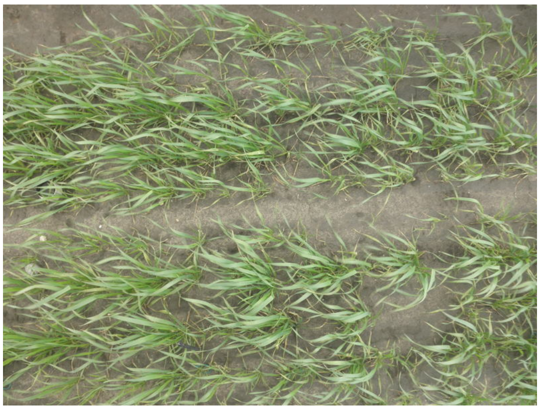

(b) 14. May 2014

(c) 2. June 2014

(d) 2. July 2014

(e) 15. July 2014

(f) 28. July 2014

Figure 41 – *Xenos* plants of plot 18 (sown on 1. April 2014) at different dates throughout the experiment.

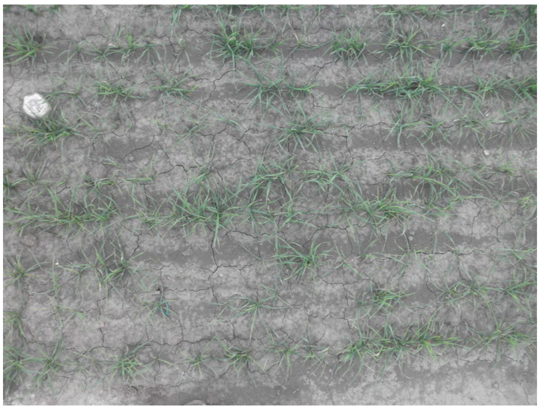

(a) 2. May 2014

(b) 14. May 2014

(c) 2. June 2014

(d) 2. July 2014

(e) 15. July 2014

(f) 28. July 2014

Figure 42 – *Capo* plants of plot 18 (sown on 1. April 2014) at different dates throughout the experiment.

12 Abstract

The Agricultural Production Systems sIMulator (APSIM) is one of the leading crop/cropping system models which is under continuous development. Due to its mechanistic nature, APSIM has the potential ability to be applied under various management and environmental conditions.

In this study, we investigated APSIM's capability of predicting growth and development of a winter (*Capo*) and a facultative (*Xenos*) wheat cultivar grown in Pannonian eastern Austria (Raasdorf, east of Vienna). The crops were sown at three sowing dates in autumn and two in spring, using a randomized split-block design with four replications. The one-year observations included soil water content, crop phenology, leaf appearance, and tiller development at weekly intervals along with destructive crop sampling for aboveground biomass and grain yield at specific dates. Meteorological data was taken from the Raasdorf station.

Pests (mice), diseases (*Puccinia striiformis*), and soil crust formation occurred on the field but were not simulated with APSIM (no appropriate sub-models). Observed rainfall and soil water content data were unreliable; soil water content prediction was poor. After calibrating the model-parameters photoperiod and vernalization, the phenological differences between the cultivars were predicted accurately. Simulation of tiller initiation for the autumn-sown treatments and leaf appearance (driven by phyllochron) matched the observations poorly. APSIM's phyllochron was nonconstant for autumn sowing dates and cultivar-independent, while observations showed constant and cultivar-dependent values. The grain yield forecast was good. Biomass predictions were solid for *Xenos* but poor for *Capo*.

APSIM was able to simulate overall phenology, biomass, and yield of the contrasting wheat cultivars well. Poor predictions were caused by wrong assumptions within the model (tiller initiation, phyllochron), the model's inability to simulate relevant processes (pests, diseases), and the lack of reliable soil water and rainfall parameterization data. We conclude from this one year study that correct modeling of all relevant processes and a solid parameterization dataset are crucial to achieve an accurate simulation of crop growth and development.

13 Zusammenfassung

APSIM (Agricultural Production Systems sIMulator) ist eines der führenden und laufend weiterentwickelten Pflanzenwachstumsmodelle. APSIM ist ein mechanistisches Modell, das potentiell unter verschiedenen Bewirtschaftungssystemen und Standortbedingungen angewandt werden kann.

In der vorliegenden Arbeit wurden mit APSIM die Simulationen einer Winter- (*Capo*) und einer Wechselweizensorte (*Xenos*) im Pannonischen Klimagebiet des Osten Österreichs (Raasdorf, östlich von Wien) untersucht. Der Anbau des einjährigen randomisierten Parzellenversuchs (Spaltblockanlage) in vierfacher Wiederholung erfolgte zu drei Terminen im Herbst und zwei im Frühjahr. Die wöchentlichen Untersuchungen beinhalteten Bodenwassergehalt, Phänologie, Anzahl von Blättern am Haupttrieb und Anzahl an Bestockungstrieben. Außerdem wurden Pflanzenproben zur Bestimmung der oberirdischen Biomasse und des Kornertrages genommen. Die meteorologischen Daten wurden von der Wetterstation in Raasdorf aufgezeichnet.

Schädlinge (Mäuse), Krankheiten (*Puccinia striiformis*) und Bodenkrustenbildung beeinflussten das Pflanzenwachstum, konnten allerdings nicht mit APSIM simuliert werden, da die entsprechenden Modelle fehlten. Die Bodenwasser- und Niederschlagsdaten waren unzuverlässig, die simulierten Bodenwassergehalte ungenau. Nachdem die modellspezifischen Parameter Photoperiode und Vernalisation kalibriert wurden konnte APSIM die phänologischen Unterschiede der beiden Weizensorten genau simulieren. Die Vorhersagen des Bestockungsbeginns der Herbstsaaten und der Entwicklung der Blattzahl am Haupttrieb (abhängig von Phyllochron) waren ungenau. APSIMs Phyllochron war sortenunabhängig und nicht konstant für Herbstsaaten, während wir sortenabhängige und konstante Werte beobachteten. Die Vorhersage des Kornertrags war insgesamt gut, die der oberirdischen Gesamtbiomasse für *Xenos* ebenfalls gut, für *Capo* ungenau.

APSIM konnte Phänologie, Biomasse und Ertrag der beiden Weizensorten erfolgreich simulieren. Unpräzise Simulationen wurden durch falsche Annahmen im Modell (Bestockungsbeginn, Phyllochron), das Fehlen wichtiger Sub-Modelle (Schädlinge, Krankheiten) und unsichere Bodenwasser- und Niederschlagsdaten verursacht. Aufgrund unserer einjährigen Ergebnisse folgern wir, dass die realitätsgetreue Modellierung aller relevanten Prozesse sowie ein korrekter Parametrisierungs-Datensatz für präzise Vorhersagen unerlässlich sind.